

# Two-stage Spatial Regression Models for Spatial Confounding

Nate Wiecha<sup>1,\*</sup> and Brian J. Reich<sup>1</sup>

<sup>1</sup>*North Carolina State University, Department of Statistics, Raleigh, North Carolina*

<sup>\*</sup>*Electronic address: nbwiecha@ncsu.edu; Corresponding author*

April 16, 2024

## Abstract

Public health data are often spatially dependent, but standard spatial regression methods can suffer from bias and invalid inference when the independent variable is associated with spatially-correlated residuals. This could occur if, for example, there is an unmeasured environmental contaminant. Geoadditive structural equation modeling (gSEM), in which an estimated spatial trend is removed from both the explanatory and response variables before estimating the parameters of interest, has previously been proposed as a solution, but there has been little investigation of gSEM's properties with point-referenced data. We link gSEM to results on double machine learning and semiparametric regression based on two-stage procedures. We propose using these semiparametric estimators for spatial regression using Gaussian processes with Matèrn covariance to estimate the spatial trends, and term this class of estimators Double Spatial Regression (DSR). We derive regularity conditions for root- $n$  asymptotic normality and consistency and closed-form variance estimation, and show that in simulations where standard spatial regression estimators are highly biased and have poor coverage, DSR can mitigate bias more effectively than competitors and obtain nominal coverage.

**Keywords**— bias reduction, double machine learning, Gaussian process, semiparametric regression, spatial confounding

# 1 Introduction

## 1.1 Spatial Confounding

Public health data are often observational and exhibit spatial dependence, such as in environmental contaminations that may spread over a geographic region (Cressie, 1993). Spatial regression methods can improve efficiency, allow proper uncertainty quantification, and enhance predictive accuracy (Cressie, 1993). However, association between explanatory variables and latent functions of space in the response model can cause bias in estimated regression coefficients, and invalid statistical inference due to poor uncertainty quantification (Reich et al., 2006). This has often been termed “spatial confounding,” and was first observed in Clayton et al. (1993), discussed further in Reich et al. (2006) and Hodges and Reich (2010), and studied in other papers such as Paciorek (2010). The analogous issue in spline models has been discussed in Rice (1986) and Wood (2017). Several recent papers (Gilbert et al., 2021; Dupont et al., 2023; Khan and Berrett, 2023) have discussed definitions, causes, and effects of spatial confounding in attempts to unify varying accounts.

Methods proposed to deal with spatial confounding aim to reduce bias in linear regression parameter estimates, such as in Marques et al. (2022), Guan et al. (2022), and Schnell and Papadogeorgou (2020). Other methods are geoadditive structural equation modeling (Thaden and Kneib, 2018), Spatial+ (Dupont et al., 2022), and a shift estimand studied in Gilbert et al. (2021) which does not assume a linear treatment effect. Geoadditive structural equation modeling (gSEM) subtracts estimated latent functions of space from the treatment and response, and regresses those residuals onto each other. Spatial+ subtracts an estimated function of space from the treatment variable and regresses the response onto those residuals. The shift estimand implemented in Gilbert et al. (2021) subtracts an estimated function of space from the treatment (in order to estimate a conditional density function) and response, but without assuming a linear and additive effect of the explanatory variable. Identifiability in gSEM, Spatial+, and the shift estimand (and our method) is typically due to independent, non-spatial variation in the treatment and response. In this situation, Gilbert et al. (2023) also showed that the standard generalized least squares (GLS), spline, and Gaussian process estimates are consistent even in some cases where they are misspecified due to spatial confounding, but noted that this does not imply variance estimates are accurate, and these estimators may converge at a rate slower than  $n^{-1/2}$ .

gSEM was initially proposed for areal spatial data, and its analogue for point-referenced spatial data has not been

studied thoroughly.<sup>1</sup> Dupont et al. (2022) states that “it is not immediately clear why the method works”; Khan and Berrett (2023) states that “the GSEM approach will result in inference...equivalent to that of a non-spatial analysis using the originally observed [variables]”; Dupont et al. (2023) states that “the bias reduction will only be successful under the assumption that the initial regressions successfully remove all spatial confounders.” The gSEM estimator has also lacked a closed-form variance estimate.

In this paper we provide connections to literature on semiparametric inference (Robinson, 1988; Andrews, 1994; Chernozhukov et al., 2018) which proves that under spatial confounding and additional regularity conditions, a class of estimators, which includes some nearly identical to gSEM, can achieve  $n^{-1/2}$ -consistency and asymptotic normality, with a consistent closed-form variance estimate, even when not removing spatial confounding exactly in initial regression estimates of spatial trends. We use Gaussian Process (GP) regression to estimate the latent functions of space, and term the application of these two-stage semiparametric estimators to address spatial confounding as Double Spatial Regression (DSR). In simulations of spatial confounding, we verify that gSEM can provide a notable bias reduction in finite samples over standard spatial and non-spatial regression, and show that new DSR estimators based on those suggested by the semiparametric literature can provide further, significant increases in performance in severe confounding scenarios.

## 1.2 Overview of related semiparametric theory

This section briefly summarizes the semiparametric literature on root- $n$  consistency and asymptotic normality of estimators similar to gSEM. More complete explanations can be found in Andrews (1994) and Chernozhukov et al. (2018). For  $i \in \{1, \dots, n\}$ , let  $Y_i \in \mathbb{R}$  be the response variable,  $A_i$  be the treatment variable, and  $\mathbf{S}_i$  be the spatial location contained in spatial domain  $\mathcal{S} \subset \mathbb{R}^d$ . A simple model is:

$$\begin{aligned} Y_i &= A_i \beta_0 + g_0(\mathbf{S}_i) + U_i \\ A_i &= m_0(\mathbf{S}_i) + V_i. \end{aligned} \tag{1}$$

For illustration in this section we ignore covariates and assume  $A_i$  is a scalar. In (1),  $\beta_0$  is the regression coefficient of interest,  $g_0$  and  $m_0$  are unknown functions treated as nuisance parameters, and  $U_i$  and  $V_i$  are error terms with finite, non-zero variance such that  $E(U_i|A_i, \mathbf{S}_i) = 0$  and  $E(V_i|\mathbf{S}_i) = 0$  for  $i = 1, \dots, n$ , not necessary Gaussian

---

<sup>1</sup>The subject of this paper is point-referenced spatial data, so we use “gSEM” to refer to its implementation described above and in Algorithm 1, not the originally-proposed areal version.

or homoskedastic. Note that it is not necessary that  $U_i \perp V_i$ : if the  $U_i$  are heteroskedastic conditional on  $A_i$ , i.e.,  $E(U_i^2|A_i) \neq E(U_i^2)$ , then the variance of  $U_i$  is affected by  $V_i$ . Denote by  $h_0(\mathbf{s}) := E(Y_i|\mathbf{S}_i = \mathbf{s})$  (marginalizing over  $A_i$ ), and let  $\eta_0$  denote the vector of functions  $(g_0, m_0)$  or  $(h_0, m_0)$ .

Model (1) can result in invalid inference due to spatial confounding if  $g_0, m_0$  result in dependence between  $\mathbf{A}$  and  $g_0(\mathbf{S})$ . For example, if  $g_0 = m_0$ , this corresponds to an unmeasured confounder which is a function of space affecting both  $Y_1, \dots, Y_n$  and  $A_1, \dots, A_n$ , and in a spatial linear mixed model, this dependence is typically ignored. For example, spatial random effects are commonly used to implement a smoother to model the unknown function  $g_0$ , but are usually marginalized into the conditional variance of  $\mathbf{Y}$  without consideration of dependence with  $\mathbf{A}$  (Paciorek, 2010). Alternatively, some basis functions used to model  $g_0$  may be collinear with  $\mathbf{A}$ , in which case penalized estimation of the coefficients on the basis functions leads to bias in estimation of  $\beta_0$  (Reich et al., 2006).

---

**Algorithm 1** Geoadditive Structural Equation Model (gSEM) estimation of  $\beta_0$

---

**Input:** Response vector  $\mathbf{Y} \in \mathbb{R}^n$ , location matrix  $\mathbf{S} \in \mathbb{R}^{n \times d}$ , treatment vector  $\mathbf{A} \in \mathbb{R}^n$

**Output:** Estimate  $\hat{\beta}_{gSEM}$  of  $\beta_0 \in \mathbb{R}$

$\hat{h}_0 \leftarrow$  Estimate of  $h_0$  from a spatial regression model for  $\mathbf{Y}$  onto  $\mathbf{S}$ , such as a spline regression

$\mathbf{R}_Y \leftarrow \mathbf{Y} - \hat{h}_0(\mathbf{S})$

$\hat{m}_0 \leftarrow$  Estimate of  $m_0$  from a spatial regression model for  $\mathbf{A}$  onto  $\mathbf{S}$ , such as a spline regression

$\mathbf{R}_A \leftarrow \mathbf{A} - \hat{m}_0(\mathbf{S})$

$\hat{\beta}_{gSEM} \leftarrow (\mathbf{R}_A^T \mathbf{R}_A)^{-1} \mathbf{R}_A^T \mathbf{R}_Y$ , i.e., obtain  $\hat{\beta}_0$  by regressing the residuals  $\mathbf{R}_Y$  onto the residuals  $\mathbf{R}_A$

**return**  $\hat{\beta}_{gSEM}$

---

The gSEM procedure is in Algorithm 1. Variance is typically estimated via bootstrap when gSEM is used in simulation studies (Guan et al., 2022; Gilbert et al., 2021). Aside from the method of estimating  $h_0$  and  $m_0$  and variance estimation, this is identical to the procedure considered in Robinson (1988). Intuitively, it is approximately orthogonalizing  $\mathbf{Y}$  and  $\mathbf{A}$  with respect to  $\mathbf{S}$  and therefore removing effects of spatial confounding.

### 1.2.1 Orthogonality of $\hat{\beta}_{gSEM}$ and nuisance parameter estimates

To study  $\hat{\beta}_{gSEM}$ 's asymptotic properties, note that  $\hat{\beta}_{gSEM}$  is equivalently defined as the solution to

$$\frac{1}{n} \sum_{i=1}^n \psi(Y_i, A_i, \mathbf{S}_i; \hat{\beta}_{gSEM}, \hat{\eta}_0) = 0$$

where  $\psi(Y_i, A_i, \mathbf{S}_i; \beta, \eta) = \{Y_i - h(\mathbf{S}_i) - \beta(A_i - m(\mathbf{S}_i))\}(A_i - m(\mathbf{S}_i))$ ,  $\eta = (h, m)$ ,  $\hat{\eta}_0 = (\hat{h}_0, \hat{m}_0)$ , and  $\hat{h}_0$  and  $\hat{m}_0$  are preliminary estimates of the nuisance parameters  $h_0$  and  $m_0$ . The score function  $\psi$  is used in [Robinson \(1988\)](#), and also studied in [Andrews \(1994\)](#) and [Chernozhukov et al. \(2018\)](#). This score function results in a form of orthogonality between  $\hat{\beta}_{gSEM}$  and  $\hat{\eta}_0$ : under the model (1), replacement of  $\eta_0$  by  $\hat{\eta}_0$  in  $\frac{1}{n} \sum_{i=1}^n E[\psi(Y_i, A_i, \mathbf{S}_i; \beta_0, \eta_0)]$  has an effect that is  $o_P(n^{-1/2})$  when  $\hat{\eta}_0$  is close to  $\eta_0$  and  $\hat{h}_0, \hat{m}_0$  each converge to their true values at  $o_P(n^{-1/4})$  rate and obey smoothness conditions, and other regularity conditions are assumed ([Andrews, 1994](#)).<sup>2</sup> Alternatively, [Chernozhukov et al. \(2018\)](#) uses the term (near-) Neyman orthogonality. Neyman orthogonality means that the Gateaux functional derivative<sup>3</sup> with respect to  $\eta$  is 0 at the true nuisance parameter values:

$$\partial_{\eta} E[\psi(Y_i, A_i, \mathbf{S}_i; \beta_0, \eta_0)][\eta - \eta_0] = 0,$$

and in the case of near-Neyman orthogonality, that it is  $o_P(n^{-1/2})$ . Similarly, this indicates that close to  $\eta_0$ , there is little effect on  $E[\psi(Y_i, A_i, \mathbf{S}_i; \beta_0, \eta_0)]$  when replacing  $\eta_0$  by its estimate. The orthogonality property means that the estimates  $\hat{h}_0$  and  $\hat{m}_0$  can converge to  $h_0$  and  $m_0$  at rates slower than  $o_P(n^{-1/2})$  and asymptotically this deviation from  $(h_0, m_0)$  does not affect the variance of  $\hat{\beta}_{gSEM}$  ([Andrews, 1994](#)).

### 1.2.2 Stochastic equicontinuity or sample splitting

The orthogonality property of  $\psi$  must be paired with a means of ensuring that estimation error of  $\eta_0$  does not cause asymptotic bias, primarily due to overfitting ([Chernozhukov et al., 2018](#)). This is achieved by a property of empirical processes called stochastic equicontinuity in [Andrews \(1994\)](#) and by sample splitting in [Chernozhukov et al. \(2018\)](#).

<sup>2</sup>Estimating the nuisance parameters using spline regression may not meet the sufficient conditions for good asymptotic behavior presented in ([Andrews, 1994](#)), which used nonparametric kernel regression estimators.

<sup>3</sup>Using the notation of [Chernozhukov et al. \(2018\)](#), the Gateaux derivative is defined as  $D_r[\eta - \eta_0] := \partial_r \left\{ E[\psi(W; \beta_0, \eta_0 + r(\eta - \eta_0))] \right\}$  for  $r \in [0, 1]$ ,  $\eta \in T$  where  $T$  is a convex subspace of a normed vector space, and  $\partial_{\eta} E[\psi(W; \beta_0, \eta_0)] := D_0[\eta - \eta_0]$ .

Stochastic equicontinuity follows from Donsker conditions (Belloni et al., 2017) which limit the complexity of  $\eta_0$  and  $\hat{\eta}_0$ . In Andrews (1994), these are primarily satisfied by placing a smoothness requirement on  $\eta_0$  and  $\hat{\eta}_0$ . In contrast, the sample-splitting approach of Chernozhukov et al. (2018) avoids requiring Donsker conditions, and therefore additional smoothness requirements. Since by using sample splitting Chernozhukov et al. (2018) allows estimation of  $\eta_0$  by essentially any machine learning model, they term their method Double Machine Learning (DML). By using cross-fitting, the DML estimators of Chernozhukov et al. (2018) still use the full sample so do not lose power. We therefore rely on Chernozhukov et al. (2018) for our theoretical analysis of an estimator similar to gSEM, and term our estimator Double Spatial Regression since we are using Double Machine Learning with spatial regression. Regularity conditions of DSR are relatively unrestrictive and interpretable using GP regression to estimate  $\eta_0$ , which is common in spatial statistics. To theoretically justify not using sample-splitting, either kernel regression estimators and the theory of Robinson (1988) should be used, or the additional smoothness requirements on  $\eta_0$  and  $\hat{\eta}_0$  from Andrews (1994) need to be satisfied, although the smoothness requirements on  $\hat{\eta}_0$  may be difficult to satisfy, except, again, for kernel regression estimators for which Andrews (1994) provides sufficient conditions justifying their use. We refer to Robinson (1988) and Andrews (1994) for the details of nonparametric kernel regression estimators considered in their papers.<sup>4</sup>

When the score function  $\psi$  has the desired orthogonality property and either stochastic equicontinuity holds or sample splitting is used, the main requirements are satisfied to justify using preliminary estimates of the spatial trends of  $\mathbf{Y}$  and  $\mathbf{A}$  in order to approximately remove confounding due to spatial location, and subject to additional regularity conditions, the resulting estimate of  $\beta_0$  will be root- $n$  consistent and asymptotically normal with a consistent, closed-form variance estimate.

## 2 Double Spatial Regression

For  $i \in \{1, \dots, n\}$ , let  $Y_i \in \mathbb{R}$  be the response variable,  $\mathbf{A}_i = (a_{i1}, a_{i2}, \dots, a_{i\ell})^T \in \mathbb{R}^\ell$  be the treatment variables,  $\mathbf{Z}_i = (z_{i1}, z_{i2}, \dots, z_{iv})^T \in \mathbb{R}^v$  be the covariates, and  $\mathbf{S}_i$  be the spatial location contained in spatial domain  $\mathcal{S} \subset \mathbb{R}^d$ .

---

<sup>4</sup>Although nonparametric Gaussian process regression also requires a choice of covariance kernel, it is different from the kernel regression estimators considered in Robinson (1988) and Andrews (1994).

The assumed model for  $i = 1, \dots, n$  and  $j = 1, \dots, \ell$  is:

$$\begin{aligned} Y_i &= \mathbf{A}_i^T \boldsymbol{\beta}_0 + \mathbf{Z}_i^T \boldsymbol{\theta}_{00} + g_0(\mathbf{S}_i) + U_i \\ A_{ij} &= \mathbf{Z}_i^T \boldsymbol{\theta}_{0j} + m_{0j}(\mathbf{S}_i) + V_{ij}, \end{aligned} \quad (2)$$

where  $Y_i$  is the response,  $A_{ij}$  is the value of treatment  $j$  for unit  $i$ ,  $\mathbf{Z}_i$  is the covariate vector for unit  $i$ , and  $\boldsymbol{\beta}_0$  is the regression coefficient vector of interest. The vectors  $\boldsymbol{\theta}_{00}, \dots, \boldsymbol{\theta}_{0\ell}$  and the collection of functions  $\eta_0 = (g_0, m_{01}, \dots, m_{0\ell})$  are all nuisance parameters.  $U_i$  and  $V_{ij}$  are error terms such that  $E(U_i | \mathbf{A}_i, \mathbf{Z}_i, \mathbf{S}_i) = E(V_{ij} | \mathbf{Z}_i, \mathbf{S}_i) = 0$  and  $\text{Var}(U_i | \mathbf{S}_i) = \sigma_{0i}^2, \text{Var}(V_{ij} | \mathbf{S}_i) = \sigma_{ji}^2$ , and  $0 < C_1 < \sigma_{0i}^2, \sigma_{ji}^2 < C_0$  for some  $0 < C_1 < C_0$  and all  $i, j$ . As in the previous section,  $U_i$  may not be independent from  $V_{ij}$  if its variance depends on the value of  $A_{ij}$ . Given  $\boldsymbol{\beta}_0, \boldsymbol{\theta}_{00}, \dots, \boldsymbol{\theta}_{0\ell}, \eta_0$ , we assume the observation vectors  $\mathbf{W}_i = (\mathbf{S}_i, \mathbf{Z}_i, \mathbf{A}_i, Y_i) \stackrel{iid}{\sim} P$  for some joint probability distribution  $P$ .

## 2.1 Double Spatial Regression algorithm

Assume  $\mathbf{Y}$  and the columns of  $\mathbf{A}$  are centered so their means are 0. We describe methods with and without cross-fitting below, which correspond to the methods in [Chernozhukov et al. \(2018\)](#) and [Andrews \(1994\)](#) respectively, applied to spatial regression. For cross-fitting, the full data set is randomly partitioned into  $K$  folds each of size  $\frac{n}{K}$ , assumed to be an integer. Let  $f_i \in \{1, \dots, K\}$  denote the fold assignment of observation  $i$ . For  $k = 1, \dots, K$ , let  $\mathbf{k} = \{i : f_i = k\}$  denote the set of indices assigned to fold  $k$  and  $\mathbf{k}^C = \{i : f_i \neq k\}$  denote the set of indices assigned to the complement of fold  $k$ . Then, for example,  $\mathbf{Y}_{\mathbf{k}}$  is the vector of elements of  $\mathbf{Y}$  assigned to the  $k$ th fold and  $\mathbf{Y}_{\mathbf{k}^C}$  is the vector of elements of  $\mathbf{Y}$  not assigned to the  $k$ th fold. For a matrix  $\mathbf{A} \in \mathbb{R}^{n \times p}$ , the elements of the matrix in the  $j$ th column are denoted  $\mathbf{A}_j$  and the elements in the  $k$ th fold and the  $j$ th column are denoted  $\mathbf{A}_{\mathbf{k},j}$ . The number of elements in fold  $k$  is denoted by  $|\mathbf{k}|$ . Denote the full sample as  $\mathbf{W}$  and the data set in fold  $k$  as  $\mathbf{W}_{\mathbf{k}}$ .

DSR uses Kriging (although other nonparametric estimators can be used) which requires a working correlation function be specified, and we use the Matérn correlation function ([Stein, 1999](#)). The Matérn correlation function is:

$$C_{\gamma, \tau}(\mathbf{S}_i, \mathbf{S}_j) := \frac{2^{1-\tau}}{\Gamma(\tau)} \left( \sqrt{2\tau} \frac{\|\mathbf{S}_i - \mathbf{S}_j\|_2}{\gamma} \right)^\tau K_\tau \left( \sqrt{2\tau} \frac{\|\mathbf{S}_i - \mathbf{S}_j\|_2}{\gamma} \right), \quad (3)$$

where  $K_\tau$  is the modified Bessel function of the second kind. The Matérn correlation function has two hyperparam-

eters:  $\gamma$  controls the range of spatial dependence and  $\tau$  controls the smoothness of the process. For matrix inputs  $\mathbf{A}$  and  $\mathbf{B}$  to a correlation function,  $C(\mathbf{A}, \mathbf{B})$  denotes the correlation matrix where the element in row  $i$  and column  $j$  equals  $C(\mathbf{A}_i, \mathbf{B}_j)$ . A variance parameter  $\omega^2$  is typically defined so that  $\omega^2 C(\mathbf{A}, \mathbf{B})$  is a covariance matrix.

Universal Kriging (Stein, 1999) is used to estimate  $g_0, m_0$ . If cross-fitting is not used, the Universal Kriging equations are:

$$\hat{g}_0(\mathbf{S}) = \hat{\omega}_0^2 C_{\hat{\gamma}_0, \hat{\tau}_0}(\mathbf{S}, \mathbf{S}) \left( \hat{\omega}_0^2 C_{\hat{\gamma}_0, \hat{\tau}_0}(\mathbf{S}, \mathbf{S}) + \hat{\sigma}_0^2 \mathbf{I} \right)^{-1} (\mathbf{Y} - \mathbf{A}^T \hat{\beta}_0 - \mathbf{Z}^T \hat{\theta}_0) \quad (4)$$

$$\hat{m}_0(\mathbf{S}) = \hat{\omega}_j^2 C_{\hat{\gamma}_j, \hat{\tau}_j}(\mathbf{S}, \mathbf{S}) \left( \hat{\omega}_j^2 C_{\hat{\gamma}_j, \hat{\tau}_j}(\mathbf{S}, \mathbf{S}) + \hat{\sigma}_j^2 \mathbf{I} \right)^{-1} (\mathbf{A}_j - \mathbf{Z}^T \hat{\theta}_j). \quad (5)$$

Note that  $\hat{\beta}_0$  is a preliminary estimate of  $\beta_0$  only. For this working prediction model we also assume homoskedasticity of all error terms, with variance parameters  $\sigma_0^2, \sigma_1^2, \dots, \sigma_\ell^2$ , and we also include the variance of the spatial processes  $\omega_0^2, \omega_1^2, \dots, \omega_\ell^2$ . To obtain universal Kriging estimates, we used the `GP` package by Guinness (2018), which estimates all covariance and slope parameters using restricted maximum likelihood (REML) and the full data set, and the Vecchia approximation (Vecchia, 1988), and scales well to large sample sizes.

If cross-fitting is used, the equations on fold  $k$  are:

$$\hat{g}_0(\mathbf{S}_{\mathbf{k}}) := \hat{\omega}_{0k}^2 C_{\hat{\gamma}_{0k}, \hat{\tau}_{0k}}(\mathbf{S}_{\mathbf{k}}, \mathbf{S}_{\mathbf{k}^C}) \left( \hat{\omega}_{0k}^2 C_{\hat{\gamma}_{0k}, \hat{\tau}_{0k}}(\mathbf{S}_{\mathbf{k}^C}, \mathbf{S}_{\mathbf{k}^C}) + \hat{\sigma}_{0k}^2 \mathbf{I} \right)^{-1} (\mathbf{Y}_{\mathbf{k}^C} - \mathbf{A}_{\mathbf{k}^C}^T \hat{\beta}_{0k} - \mathbf{Z}_{\mathbf{k}^C}^T \hat{\theta}_{0k}) \quad (6)$$

$$\hat{m}_{0j}(\mathbf{S}_{\mathbf{k}}) := \hat{\omega}_{jk}^2 C_{\hat{\gamma}_{jk}, \hat{\tau}_{jk}}(\mathbf{S}_{\mathbf{k}}, \mathbf{S}_{\mathbf{k}^C}) \left( \hat{\omega}_{jk}^2 C_{\hat{\gamma}_{jk}, \hat{\tau}_{jk}}(\mathbf{S}_{\mathbf{k}^C}, \mathbf{S}_{\mathbf{k}^C}) + \hat{\sigma}_{0jk}^2 \mathbf{I} \right)^{-1} (\mathbf{A}_{\mathbf{k}^C, j} - \mathbf{Z}_{\mathbf{k}^C}^T \hat{\theta}_{jk}), \quad (7)$$

where the parameters are as before but now the subscript  $k$  indicates an estimate obtained for prediction on fold  $k$ , obtained as before using REML and the Vecchia approximation on  $\mathbf{k}^C$ , the data not in fold  $k$ . For large datasets GP covariance parameters can be selected once using the entire dataset and the same values used for cross-fitting with each fold. This could degrade performance slightly, since for each fold, the response values being predicted were used to select covariance parameters. However, this approach is much faster, so we use this approach in simulations. Predictions are combined across folds to obtain  $\hat{g}_0(\mathbf{S})$  and  $\hat{m}_0(\mathbf{S})$ . If cross-fitting is used, different runs will produce different estimates of  $\beta_0$  due to random sample splitting. Fuhr et al. (2024) recommends using enough folds that the estimates are relatively stable, and pick the median point and variance estimates out of as large a number of estimates as is feasible.

The residuals from the Kriging fit are then used to compute  $\hat{\beta}_{DSR}$  and its variance estimate. The expressions for the estimator and its variance estimate are the same with and without cross-fitting. Letting  $\hat{\mathbf{V}}_j = \mathbf{A}_j - \hat{m}_j(\mathbf{S})$ , and  $\hat{\mathbf{J}} = (\hat{\mathbf{V}}^T \mathbf{A})^{-1}$ :

$$\begin{aligned} \hat{\beta}_{DSR} &= \hat{\mathbf{J}} \hat{\mathbf{V}}^T (\mathbf{Y} - \mathbf{Z}^T \hat{\theta}_0 - \hat{g}(\mathbf{S})) \\ \widehat{Var}(\hat{\beta}_{DSR}) &= \hat{\mathbf{J}} \left( \sum_{i=1}^n \left[ \hat{\mathbf{V}}_i (Y_i - \mathbf{A}_i^T \hat{\beta}_{DSR} - \mathbf{Z}_i^T \hat{\theta}_0 - \hat{g}(\mathbf{S}_i)) \right] \left[ \hat{\mathbf{V}}_i (Y_i - \mathbf{A}_i^T \hat{\beta}_{DSR} - \mathbf{Z}_i^T \hat{\theta}_0 - \hat{g}(\mathbf{S}_i)) \right]^T \right) \hat{\mathbf{J}}^T \end{aligned} \quad (8)$$

which are the estimators provided in [Chernozhukov et al. \(2018\)](#).

Cross-fitting is used in [Chernozhukov et al. \(2018\)](#) to avoid requiring Donsker conditions on the complexity of the estimators of the unknown functions of space. In [Chernozhukov et al. \(2018\)](#), this is primarily to allow the dimension of the input data vectors to the unknown functions to grow with  $n$ . Since that does not apply to spatial regression, where the spatial domain does not increase in dimension with  $n$ , cross fitting may not be necessary. [Andrews \(1994\)](#) provides sufficient conditions to forego cross-fitting, namely that both  $\eta_0$  and  $\hat{\eta}_0$  obey an additional smoothness condition (the latter with high probability). The required results for GP regression with Matèrn kernel and hyperparameters estimated via REML are not established to our knowledge, so cross-fitting could be skipped with additional assumptions about  $\eta_0$  and  $\hat{\eta}_0$ .

Code implementing DSR estimators can be found at:

<https://github.com/nbwiecha/Double-Spatial-Regression>.

## 2.2 Double Spatial Regression algorithm for theoretical analysis

While the previous algorithm is practical and performs well in simulations, limited theoretical analysis is possible. Root- $n$  consistency of  $\hat{\beta}_{DSR}$  and asymptotic normality of  $\widehat{Var}(\hat{\beta}_{DSR})^{-1/2}(\hat{\beta}_{DSR} - \beta_{DSR})$  requires convergence of the estimates from (6) and (7) at rates of  $o_P(n^{-1/4})$ , along with correct model specification and more standard regularity conditions ([Chernozhukov et al., 2018](#)). Since the learning rate for nonparametric regression estimates obtained by a Gaussian Process using a Matèrn kernel, with parameters estimated by REML and with errors in the observations, is not established to our knowledge, we cannot derive explicit conditions on  $\eta_0$  under which  $\hat{\beta}_{DSR}$  has the desired asymptotic properties.

In this section, we consider a modified algorithm that is more similar to gSEM and the estimator in [Robinson](#)

---

**Algorithm 2** DSR estimation of  $\beta_0$  with cross-fitting

---

**Input:** Response vector  $\mathbf{Y} \in \mathbb{R}^n$ , location matrix  $\mathbf{S} \in \mathbb{R}^{n \times 2}$ , treatment matrix  $\mathbf{A} \in \mathbb{R}^{n \times \ell}$ , covariate matrix  $\mathbf{Z} \in \mathbb{R}^{n \times m}$ .

**Output:** Estimate  $\hat{\beta}_{DSR}$  of  $\beta_0 \in \mathbb{R}^{\ell \times 1}$  and estimate  $\widehat{Var}(\hat{\beta}_{DSR})$  of  $Var(\hat{\beta}_{DSR}) \in \mathbb{R}^{\ell \times \ell}$   
Partition the data into  $K$  random folds so that the size of each fold is  $\frac{n}{K}$ .

**for**  $k = 1, \dots, K$  **do**

Obtain  $\hat{\beta}_{0k}, \hat{\theta}_{0k}, \dots, \hat{\theta}_{\ell k}, \hat{\gamma}_{0k}, \dots, \hat{\gamma}_{\ell k}, \hat{\tau}_{0k}, \dots, \hat{\tau}_{\ell k}, \hat{\sigma}_{0k}, \dots, \hat{\sigma}_{\ell k}$  by REML using GpGp.

Obtain  $\hat{g}(\mathbf{S}_{\mathbf{k}})$  by (6) (approximated by GpGp).

$\hat{\mathbf{Y}}_{\mathbf{k}} \leftarrow \mathbf{Z}_{\mathbf{k}}^T \hat{\theta}_{0k} + \hat{g}(\mathbf{S}_{\mathbf{k}}); \hat{\mathbf{Y}}_{\mathbf{k}} \in \mathbb{R}^{|\mathbf{k}|}$

**for**  $j = 1, \dots, \ell$  **do**

Obtain  $\hat{m}_j(\mathbf{S}_{\mathbf{k}})$  by (7) (approximated by GpGp).

$\hat{\mathbf{A}}_{\mathbf{k},j} \leftarrow \mathbf{Z}_{\mathbf{k}}^T \hat{\theta}_{jk} + \hat{m}_j(\mathbf{S}_{\mathbf{k}}); \hat{\mathbf{D}}_{\mathbf{k}} \in \mathbb{R}^{|\mathbf{k}|}$

**end for**

**end for**

Combine the estimates from each fold to obtain  $\hat{\mathbf{Y}} \in \mathbb{R}^n, \hat{\mathbf{D}} \in \mathbb{R}^{n \times \ell}$

$\hat{\mathbf{V}} \leftarrow \mathbf{A} - \hat{\mathbf{A}}$

$\hat{\mathbf{J}} \leftarrow (\hat{\mathbf{V}}^T \mathbf{A})^{-1}$

$\hat{\beta}_{DSR} \leftarrow \hat{\mathbf{J}} \hat{\mathbf{V}}^T (\mathbf{Y} - \hat{\mathbf{Y}}); \hat{\beta}_{DSR} \in \mathbb{R}^{\ell}$

$\widehat{Var}(\hat{\beta}_{DSR}) \leftarrow \hat{\mathbf{J}} \left( \sum_{i=1}^n \left[ -\hat{\mathbf{V}}_i \mathbf{A}_i^T \hat{\beta}_{DSR} + \hat{\mathbf{V}}_i (Y_i - \hat{Y}_i) \right] \left[ -\hat{\mathbf{V}}_i \mathbf{A}_i^T \hat{\beta}_{DSR} + \hat{\mathbf{V}}_i (Y_i - \hat{Y}_i) \right]^T \right) \hat{\mathbf{J}}^T$

**return**  $\hat{\beta}_{DSR}, \widehat{Var}(\hat{\beta}_{DSR})$

---

---

**Algorithm 3** DSR estimation of  $\beta_0$  without cross-fitting

---

**Input:** Response vector  $\mathbf{Y} \in \mathbb{R}^n$ , location matrix  $\mathbf{S} \in \mathbb{R}^{n \times 2}$ , treatment matrix  $\mathbf{A} \in \mathbb{R}^{n \times \ell}$ , covariate matrix  $\mathbf{Z} \in \mathbb{R}^{n \times m}$ .

**Output:** Estimate  $\hat{\beta}_{DSR}$  of  $\beta_0 \in \mathbb{R}^{\ell \times 1}$  and estimate  $\widehat{Var}(\hat{\beta}_{DSR})$  of  $Var(\hat{\beta}_{DSR}) \in \mathbb{R}^{\ell \times \ell}$

Obtain  $\hat{\beta}_0, \hat{\theta}_0, \dots, \hat{\theta}_{\ell}, \hat{\gamma}_0, \dots, \hat{\gamma}_{\ell}, \hat{\tau}_0, \dots, \hat{\tau}_{\ell}, \hat{\omega}_0^2, \dots, \hat{\omega}_{\ell}^2, \hat{\sigma}_0^2, \dots, \hat{\sigma}_{\ell}^2$  by REML using GpGp.

$\hat{g}(\mathbf{S})$  obtained by (4) (approximated by GpGp).

**for**  $j = 1, \dots, \ell$  **do**

$\hat{m}_j(\mathbf{S})$  obtained by (5) (approximated by GpGp).

$\hat{\mathbf{A}}_j \leftarrow \mathbf{Z}^T \hat{\theta}_j + \hat{m}_j(\mathbf{S}); \hat{\mathbf{A}} \in \mathbb{R}^n$

**end for**

$\hat{\mathbf{V}} \leftarrow \mathbf{A} - \hat{\mathbf{A}}$

$\hat{\mathbf{J}} \leftarrow (\hat{\mathbf{V}}^T \mathbf{A})^{-1}$

$\hat{\beta}_{DSR} \leftarrow \hat{\mathbf{J}} \hat{\mathbf{V}}^T (\mathbf{Y} - \mathbf{Z}^T \hat{\theta}_0 - \hat{g}(\mathbf{S})); \hat{\beta}_{DSR} \in \mathbb{R}^{\ell}$

$\widehat{Var}(\hat{\beta}_{DSR}) \leftarrow \hat{\mathbf{J}} \left( \sum_{i=1}^n \left[ \hat{\mathbf{V}}_i (Y_i - \mathbf{A}_i^T \hat{\beta}_{DSR} - \mathbf{Z}_i^T \hat{\theta}_0 - \hat{g}(\mathbf{S}_i)) \right] \left[ \hat{\mathbf{V}}_i (Y_i - \mathbf{A}_i^T \hat{\beta}_{DSR} - \mathbf{Z}_i^T \hat{\theta}_0 - \hat{g}(\mathbf{S}_i)) \right]^T \right) \hat{\mathbf{J}}^T$

**return**  $\hat{\beta}_{DSR}, \widehat{Var}(\hat{\beta}_{DSR})$

---

(1988), which allows derivation of explicit regularity conditions by using the results in Chernozhukov et al. (2018) on DML partially linear regression and Eberts and Steinwart (2013) on GP regression learning rates. For theoretical analysis, we return to the simpler model (1) considered in Section 1 and assume there is only one treatment  $\mathbf{A}$  and no covariates. For the theoretical results below, we use a random spatial design, but our empirical results verify that the proposed method can perform well if the  $\mathbf{S}_i$  are defined deterministically.

For theoretical analysis we consider the limit of  $C_{\gamma,\tau}(\mathbf{S}_i, \mathbf{S}_j)$  as  $\tau \rightarrow \infty$ , which yields the Gaussian correlation function (Rasmussen and Williams, 2005):

$$C_{\gamma}(\mathbf{S}_i, \mathbf{S}_j) := \exp\left(-\frac{\|\mathbf{S}_i - \mathbf{S}_j\|_2^2}{2\gamma^2}\right).$$

Note that DSR only requires the true functions in  $\eta_0$  to satisfy a smoothness criterion described in Section 2.3, and does not require that they reside in the reproducing kernel Hilbert space generated by the chosen kernel.

Denote by  $h(\mathbf{S}_i)$  the conditional expectation  $E(Y_i|\mathbf{S}_i)$  (note that this does not depend on  $A_i$ ). On each fold  $k$ , Kriging (Stein, 1999) is used to obtain cross-fitted estimates for  $h_0(\mathbf{S}_{\mathbf{k}})$  and  $m_0(\mathbf{S}_{\mathbf{k}})$ , denoted  $\hat{h}_0(\mathbf{S}_{\mathbf{k}})$ , and  $\hat{m}_0(\mathbf{S}_{\mathbf{k}})$ ,

$$\hat{h}_0(\mathbf{S}_{\mathbf{k}}) := C_{\gamma_{0k}}(\mathbf{S}_{\mathbf{k}}, \mathbf{S}_{\mathbf{k}^C}) \left( C_{\gamma_{0k}}(\mathbf{S}_{\mathbf{k}^C}, \mathbf{S}_{\mathbf{k}^C}) + |\mathbf{k}^C| \lambda_{0k} \mathbf{I} \right)^{-1} \mathbf{Y}_{\mathbf{k}^C} \quad (9)$$

$$\hat{m}_0(\mathbf{S}_{\mathbf{k}}) := C_{\gamma_{1k}}(\mathbf{S}_{\mathbf{k}}, \mathbf{S}_{\mathbf{k}^C}) \left( C_{\gamma_{1k}}(\mathbf{S}_{\mathbf{k}^C}, \mathbf{S}_{\mathbf{k}^C}) + |\mathbf{k}^C| \lambda_{1k} \mathbf{I} \right)^{-1} \mathbf{X}_{\mathbf{k}^C, j}. \quad (10)$$

For each fold, the simple Kriging predictions (9) and (10) are used to separately obtain estimates  $\hat{h}_0(\mathbf{S}_{\mathbf{k}})$  and  $\hat{m}_0(\mathbf{S}_{\mathbf{k}})$ . Denote the data in fold  $k$  by  $\mathbf{W}_{\mathbf{k}}$  and the observations in the complement of fold  $k$  by  $\mathbf{W}_{\mathbf{k}^C}$ ; the data in  $\mathbf{W}_{\mathbf{k}^C}$  are used to estimate the nuisance functions evaluated at the locations corresponding to  $\mathbf{W}_{\mathbf{k}}$ . The hyperparameters  $\lambda_{0k}, \dots, \lambda_{1k}$  control regularization and are restricted to  $(0, 1]$ . For the purpose of theoretical analysis,  $\lambda_{0k}, \dots, \lambda_{1k}, \gamma_{0k}, \dots, \gamma_{1k}$  are selected using a training-validation split of  $\mathbf{W}_{\mathbf{k}^C}$  (Eberts and Steinwart, 2013); they depend on  $k$  because our theoretical analysis requires that they are selected each time predictions are obtained (i.e., on each fold). The  $\lambda_{0k}$  and  $\lambda_{1k}$  parameters play similar roles to the variance of i.i.d. error terms in standard spatial regression, but are considered hyperparameters to be tuned rather than a parameter of the model. The data in  $\mathbf{W}_{\mathbf{k}^C}$  is split in two halves, a “training” half and a “validation” half. For each possible combination of hyperparameters ( $\lambda$  and  $\gamma$ ) considered, the training half of  $\mathbf{W}_{\mathbf{k}^C}$  is used to obtain predictions on the validation half of  $\mathbf{W}_{\mathbf{k}^C}$ . The pair of

hyperparameters with lowest mean squared error (MSE) on the validation half of  $\mathbf{W}_{\mathbf{k}^C}$  is selected for estimating  $\eta_0$  evaluated at the locations corresponding to the data in  $\mathbf{W}_{\mathbf{k}}$  (Eberts and Steinwart, 2013).

Additional technical requirements not listed in Algorithm 4, but which are required for derivation of regularity conditions in Section 2.3, relate to scaling of the data and clipping of the estimates  $\hat{h}_0, \hat{m}_0$ . If the  $U_i$  are bounded, then  $\hat{h}_0$  should be “clipped” so that  $\hat{h}_0 \in [-M_0, M_0]$ ,  $M_0 > 0$ , where by assumption  $Y_i \in [-M_0, M_0]$  for all  $i$ . If the  $U_i$  are alternatively assumed normally distributed, then the data should be scaled so that  $|h_0| \leq 1$ , and  $\hat{h}_0$  should be “clipped” so that  $|\hat{h}_0| \leq \min\{1, 4\sqrt{C_0}\sqrt{\ln(n)}\}$  for some  $C_0 > 0$  that exceeds  $\text{Var}(U_i|\mathbf{S}_i) \forall \mathbf{S}_i \in \mathcal{S}$ . Similar scaling and trimming should likewise be carried out for the  $A_i$  and corresponding  $V_i$ .

Letting  $\hat{\mathbf{V}}$  be defined as before, the DSR estimators are:

$$\begin{aligned}\hat{\beta}_0 &= (\hat{\mathbf{V}}^T \hat{\mathbf{V}})^{-1} \hat{\mathbf{V}}^T (\mathbf{Y} - \hat{h}(\mathbf{S})) \\ \widehat{\text{Var}}(\hat{\beta}_0) &= (\hat{\mathbf{V}}^T \hat{\mathbf{V}})^{-2} \left( \sum_{i=1}^n \left[ -\hat{V}_i^2 \hat{\beta}_0 + \hat{V}_i (Y_i - \hat{h}(\mathbf{S}_i)) \right]^2 \right),\end{aligned}\tag{11}$$

which are again the estimators from Chernozhukov et al. (2018).

### 2.3 Double Spatial Regression regularity conditions

This section describes the regularity conditions for DSR as implemented in Algorithm 4. Our theoretical analysis uses the results on convergence rates of GP regression from Eberts and Steinwart (2013) and asymptotic properties of DML partially linear regression from Chernozhukov et al. (2018) to obtain explicit regularity conditions on the latent functions of space  $h_0$  and  $m_0$  under which DSR is root- $n$  asymptotically normal and consistent. The technical requirements described at the end of subsection 2.2 related to scaling the data, and clipping the fitted functions should be followed for the regularity conditions to apply. The observations  $\mathbf{W}_i = (Y_i, A_i, \mathbf{S}_i)$  are assumed to be i.i.d. from a probability distribution  $P$  with density function  $p(w)$ , and for a function  $f$ ,  $\|f\|_{P,q} := \left\{ \int |f(w)|^q p(w) dw \right\}^{1/q}$ . As before the function  $h_0(\mathbf{s}) = E(Y_i|\mathbf{S}_i = \mathbf{s})$ .

To provide intuition on Assumption A6 below, the following explanation of Besov spaces is paraphrased from Eberts and Steinwart (2013). Denote the  $\zeta$ -th weak derivative  $\partial^{(\zeta)}$  for a multi-index  $\zeta = (\zeta_1, \zeta_2, \dots, \zeta_d) \in \mathbb{N}^d$  with

---

**Algorithm 4** Double Spatial Regression estimation of  $\beta_0$  for theoretical study
 

---

**Input:** Centered response vector  $\mathbf{Y} \in \mathbb{R}^n$ , location matrix  $\mathbf{S} \in \mathbb{R}^{n \times d}$ , centered treatment vector  $\mathbf{A} \in \mathbb{R}^n$ .

**Output:** Estimate  $\hat{\beta}_0$  of  $\beta_0 \in \mathbb{R}$  and estimate  $\widehat{Var}(\hat{\beta}_0)$  of  $Var(\hat{\beta}_0) \in \mathbb{R}$

Randomly partition the data into  $K$  folds so that the size of each fold is  $\frac{n}{K}$ .

**for**  $k = 1, \dots, K$  **do**

Select the hyperparameters  $\gamma_{0,k}, \lambda_{0,k} \in \mathbb{R}$  by a training-validation approach, using data in  $\mathbf{k}^C$ . The value of  $\lambda_{0k}$  is selected from an evenly-spaced grid of  $\frac{1}{2n}$  values in  $(0, 1]$ , the lengthscale  $\gamma_{0k}$  is selected from an evenly-spaced grid of  $\frac{1}{2n^{-1/4}}$  values in  $(0, 1]$ .

$$\hat{h}_0(\mathbf{S}_{\mathbf{k}}) \leftarrow C_{\gamma_{0k}}(\mathbf{S}_{\mathbf{k}}, \mathbf{S}_{\mathbf{k}^C}) \left( C_{\gamma_{0k}}(\mathbf{S}_{\mathbf{k}^C}, \mathbf{S}_{\mathbf{k}^C}) + |\mathbf{k}^C| \lambda_{0k} \mathbf{I} \right)^{-1} \mathbf{Y}_{\mathbf{k}^C}$$

Select the hyperparameters  $\gamma_{1,k}, \lambda_{1,k} \in \mathbb{R}$  by a training-validation approach, using data in  $\mathbf{k}^C$ . The value of  $\lambda_{1k}$  is selected from an evenly-spaced grid of  $\frac{1}{2n}$  values in  $(0, 1]$ , the lengthscale  $\gamma_{1k}$  is selected from an evenly-spaced grid of  $\frac{1}{2n^{-1/4}}$  values in  $(0, 1]$ .

$$\hat{m}_0(\mathbf{S}_{\mathbf{k}}) \leftarrow C_{\gamma_{1k}}(\mathbf{S}_{\mathbf{k}}, \mathbf{S}_{\mathbf{k}^C}) \left( C_{\gamma_{1k}}(\mathbf{S}_{\mathbf{k}^C}, \mathbf{S}_{\mathbf{k}^C}) + |\mathbf{k}^C| \lambda_{1k} \mathbf{I} \right)^{-1} \mathbf{A}_{\mathbf{k}^C}$$

**end for**

Combine the predictions from each fold to obtain  $\hat{h}_0(\mathbf{S}) \in \mathbb{R}^n$ ,  $\hat{m}_0(\mathbf{S}) \in \mathbb{R}^n$

$$\hat{\mathbf{V}} \leftarrow \mathbf{A} - \hat{m}(\mathbf{S})$$

$$\hat{\mathbf{J}} \leftarrow (\hat{\mathbf{V}}^T \hat{\mathbf{V}})^{-1}$$

$$\hat{\beta}_0 \leftarrow \hat{\mathbf{J}} \hat{\mathbf{V}}^T (\mathbf{Y} - \hat{h}(\mathbf{S}))$$

$$\widehat{Var}(\hat{\beta}_0) \leftarrow \hat{\mathbf{J}} \left( \sum_{i=1}^n \left[ -\hat{V}_i^2 \hat{\beta}_0 + \hat{V}_i (Y_i - \hat{h}(\mathbf{S}_i)) \right]^2 \right) \hat{\mathbf{J}}^T$$

**return**  $\hat{\beta}_0, \widehat{Var}(\hat{\beta}_0)$

---

$|\zeta| = \sum_{i=1}^d \zeta_i$ . With regard to a measure  $\nu$ , the Sobolev space  $W_p^\alpha(\nu)$  is defined as:

$$W_p^\alpha(\nu) := \{f \in L_p(\nu) : \partial^{(\zeta)} f \in L_p(\nu) \text{ exists for all } \zeta \in \mathbb{N}^d \text{ with } |\zeta| < \alpha\}.$$

Loosely speaking,  $W_p^\alpha(\nu)$  is the space of functions with  $\alpha$  weak derivatives, which all must have finite  $L_p(\nu)$  norm. We refer to [Eberts and Steinwart \(2013\)](#) for a full definition of Besov spaces  $B_{p,q}^\alpha$ , but Besov spaces provide a finer scale of smoothness than the integer-ordered Sobolev spaces, and Sobolev spaces are contained in the Besov spaces:

$$W_p^\alpha(\mathbb{R}^d) \subset B_{p,q}^\alpha(\mathbb{R}^d)$$

for  $\alpha \in \mathbb{N}$ ,  $p \in (1, \infty)$ ,  $\max\{p, 2\} \leq q \leq \infty$ .

The further assumptions for DSR are:

A1) The data are generated by (1).

A2) The errors  $U_i, V_i$  are such that  $E(U_i|A_i, \mathbf{S}_i) = E(V_i|\mathbf{S}_i) = 0$ , with variances  $\sigma_{0i}, \sigma_{1i}$  respectively such that  $0 < C_1 < \sigma_{0i}^2, \sigma_{1i}^2 < C_0$  for some  $0 < C_1 < C_0$  and for all  $i = 1, \dots, n$ . Also,  $E(U_i^2 V_i^2)$  is bounded away from 0. The errors  $U_i$  and  $V_i$  are either bounded in some interval or are normally distributed.

A3) The spatial locations  $\mathbf{S}_i$  reside in a region  $\mathcal{S}$  contained in a unit ball in  $\mathbb{R}^d$ , and the boundary of  $\mathcal{S}$  has  $P$ -probability 0. The marginal distribution  $P_S$  of  $\mathbf{S}_i$  (derived from  $P$ ) is absolutely continuous on  $\mathcal{S}$  and has a density  $p_S \in L_q(\mathbb{R}^d)$  for some  $q \geq 1$ .

A4) The marginal distribution  $P_A$  of the treatments  $A_i$  has at least 5 finite moments.

A5) If the errors  $U_i$  are bounded, then  $h_0$  is such that  $Y_i \in [-M_0, M_0]$  for all  $i = 1, \dots, n$  and for some  $M_0 > 0$ , and if  $U_i$  are normally distributed then  $h_0 \in [-1, 1]$ . Similarly, if the  $V_i$  are bounded, then  $m_0$  is such that  $A_i \in [-M_1, M_1]$  for all  $i = 1, \dots, n$  and some  $M_1 > 0$ , and if  $V_i$  are normally distributed then  $m_0 \in [-1, 1]$ .

A6) The function  $m_0$  resides in the Besov space  $B_{2s,\infty}^{\alpha_A}$  where the smoothness order  $\alpha_A > \frac{d}{2}$ ,  $\alpha_A \geq 1$ , and  $\frac{1}{s} + \frac{1}{q} = 1$  and  $s \geq 1$ , and  $h_0$  resides in the Besov space  $B_{2s,\infty}^{\alpha_Y}$  where the smoothness order  $\alpha_Y > \frac{d^2}{4\alpha_A}$  and  $\alpha_Y \geq 1$ . Furthermore,  $h_0, m_0 \in L_2(\mathbb{R}^d)$ .

A stronger, but more interpretable alternative to assumption A6 is that  $m_0$  resides in the integer-order Sobolev space  $W_{2s}^{\alpha_A}$  and  $h_0$  resides in the integer-order Sobolev space  $W_{2s}^{\alpha_Y}$ , where  $\alpha_A$  and  $\alpha_Y$  are integers, and  $\alpha_A > \frac{d}{2}$ ,  $\alpha_A \geq 1$ ,  $\alpha_Y \geq 1$ , and  $\alpha_Y > \frac{d^2}{4\alpha_A}$  (and all functions are still  $L_2$ -integrable). In the common scenario  $d = 2$ , this reduces to the requirement that  $\alpha_A$  and  $\alpha_Y$  must be greater than 1, which for integer-ordered Sobolev spaces, loosely means that both  $h_0$  and  $m_0$  have at least two partial derivatives. Per the discussion following Theorem 3.6 in [Eberts and Steinwart \(2013\)](#), the distributions of  $U_i, V_i$  can follow other light-tailed distributions aside from normal.

Theorem 1 states that DSR is asymptotically normal and consistent under the above assumptions.

**Theorem 1.** *If Assumptions A1 – A6 are met, and  $\hat{\beta}_0$  and  $\widehat{Var}(\hat{\beta}_0)$  are obtained by Algorithm 4, and estimated functions are trimmed as discussed above, then*

$$\begin{aligned} \sigma^{-1}\sqrt{n}(\hat{\beta}_0 - \beta_0) &\xrightarrow{D} N(0, 1), \text{ and} \\ \widehat{Var}(\hat{\beta}_0)^{-1/2}(\hat{\beta}_0 - \beta_0) &\xrightarrow{D} N(0, 1), \end{aligned}$$

where  $\sigma^2 = E[V_i^2]^{-1}E[U_i^2V_i^2](E[V_i^2]^{-1})$  is the approximate variance of  $\hat{\beta}_0$ .

**Sketch of proof 1.** By Theorem 4.1 in [Chernozhukov et al. \(2018\)](#), the result of Theorem 1 requires that  $\|m_0 - \hat{m}_0\|_{P,2} \times \|h_0 - \hat{h}_0\|_{P,2} \leq \delta_n n^{-1/2}$  and  $\|m_0 - \hat{m}_0\|_{P,2}^2 \leq \delta_n n^{-1/2}$ , for some sequence  $\delta_n \rightarrow 0$ ,  $\delta_n \geq n^{-1/2}$ , with probability converging to 1. For estimates of an unknown function  $f$  obtained by a Gaussian Process posterior mean with Gaussian kernel, and hyperparameters selected using a training-validation approach, the near-optimal convergence rate  $\|\hat{f} - f\|_{P,2} \leq Qn^{-\frac{\alpha}{2\alpha+d} + \xi}$ , for all  $\xi > 0$  and with probability converging to 1, where  $Q > 0$  is a constant, and  $\alpha \geq 1$  is the smoothness of  $f$ , is established by [Eberts and Steinwart \(2013\)](#). Combining these results, we find that fast-enough convergence rates of  $\hat{m}_0$  and  $\hat{h}_0$  to  $m_0$  and  $h_0$  are obtained if  $\alpha_A > \frac{d}{2}$  and  $\alpha_A \geq 1$ , and  $\alpha_Y > \frac{d^2}{4\alpha_A}$  and  $\alpha_Y \geq 1$ .

*The full proof is in the appendix.*

In addition, Remark 4.2 of [Chernozhukov et al. \(2018\)](#) states that if the error terms  $U_i$  are homoskedastic conditional on  $A_i$ , then  $\sigma^2 = E(V^2)^{-1}E(U^2)$ , and  $\hat{\beta}_0$  achieves the bound on semiparametric efficiency for  $\beta_0$ .

## 3 Simulation Study

### 3.1 Simulation study outline

In this simulation study, we evaluate several estimators’ performance in finite samples. We include both the DSR estimator presented in Section 2.1 with cross-fitting (Algorithm 2) and without cross-fitting (Algorithm 3), and the “theoretical DSR” estimator studied in Section 2.2 (Algorithm 4) and an alternative version of Algorithm 4 without cross-fitting. Although theoretical DSR requires the lengthscales  $\gamma$  to be selected from a grid of size  $\frac{1}{2n^{-1/4}}$  values for asymptotic properties to hold, we use a grid of size  $\frac{1}{2n^{-1/2}}$  to improve finite-sample performance. DSR estimators with cross-fitting used  $K = 5$  folds. We also implemented DSR without cross-fitting, and using spline regression to estimate latent functions of space, to isolate differences with gSEM. Comparison methods were the geospatial structural equation model (gSEM) of Thaden and Kneib (2018), implemented using splines for geostatistical data (Algorithm 1), Spatial+ of Dupont et al. (2022), the naive (unadjusted for spatial confounding) spatial linear mixed model (LMM), spline regression using generalized cross-validation (GCV) and REML to estimate the smoothing parameter for a smooth function of space (Wood, 2017), and ordinary least squares (OLS). The nonparametric shift estimator studied in Gilbert et al. (2021) was tried but was not able to obtain estimates in most scenarios we used; its results are only included in Table A9, without a variance estimate, which required bootstrapping estimates that were computationally expensive relative to other methods considered. Spatial+ removes a fitted spatial surface from the treatment variable, and then performs thin-plate spline regression of the outcome onto the residuals. The naive spatial linear mixed model (LMM) is fitted using the R package GpGp (Guinness, 2018) and spline models fit using the R package mgcv (Wood, 2011). Simulations were carried out in R version 4.2.1 (R Core Team, 2023).

### 3.2 Data generating process

For our main simulations, we generate data from Gaussian processes in order to control the smoothness of the generated processes. Observations were drawn from multivariate normal distributions with selected covariances, equivalent to drawing a random function from a Gaussian process prior with that kernel and evaluating it at those points. DSR adjusts for fixed functions of space, and this data generating process is equivalent to randomly drawing a new fixed function of space from a prior distribution in each Monte Carlo iteration. The data-generating process

for the main simulations is similar to that used in [Marques et al. \(2022\)](#):  $\mathbf{Y} \sim N(\beta_0 \mathbf{A} + \mathbf{U}, \sigma_Y^2 \mathbf{I})$ ,

$$\begin{bmatrix} \mathbf{A} \\ \mathbf{U} \end{bmatrix} \sim N \left( \begin{bmatrix} \mathbf{0} \\ \mathbf{0} \end{bmatrix}, \begin{bmatrix} \Sigma_{\mathbf{A}} + \sigma_A^2 \mathbf{I} & \rho \Sigma_{\mathbf{A}}^{1/2} (\Sigma_{\mathbf{U}}^{1/2})^T \\ \rho \Sigma_{\mathbf{U}}^{1/2} (\Sigma_{\mathbf{A}}^{1/2})^T & \Sigma_{\mathbf{U}} \end{bmatrix} \right),$$

where  $\mathbf{Y}, \mathbf{A}, \mathbf{U} \in \mathbb{R}^n$ ,  $\Sigma_{\mathbf{A}}$  and  $\Sigma_{\mathbf{U}}$  are spatial correlation matrices in  $\mathbb{R}^{n \times n}$ , and  $\rho \in [-1, 1]$ .  $\mathbf{A}$  is the independent variable,  $\beta_0$  is the parameter of interest, and  $\mathbf{U}$  is an unobserved confounder. We used two spatial covariance matrices for both  $\Sigma_{\mathbf{A}}$  and  $\Sigma_{\mathbf{U}}$  that generate realizations of smooth and rough functions of space:

- Rough: Matèrn covariance function with smoothness parameter  $\tau = 1.5$ , range parameter  $\gamma = 0.2$ , and variance 1
- Smooth: Gneiting covariance function ([Schlather et al., 2015](#)) with range parameter  $\gamma = 0.2$ , and variance 1

The Gneiting covariance function approximates a Gaussian covariance function but is less prone to producing computationally singular covariance matrices ([Schlather et al., 2015](#)). These were both used as implemented in the R package `geoR` ([Ribeiro Jr et al., 2023](#)).

For our main simulations,  $n = 1000$ ,  $\rho = 0.5$ ,  $\sigma_A^2 = 0.1^2$ ,  $\sigma_Y^2 = 1$ , and  $\beta_0 = 0.5$ . The settings were chosen to be a challenging case of spatial confounding, since the relative lack of i.i.d. variance in  $\mathbf{A}$  provides less unconfounded variation in the treatment, causing severe spatial confounding bias in finite samples. Spatial locations were randomly sampled uniformly from  $[0, 1]^2$ .

Several additional simulated scenarios generated data subject to heteroskedasticity, nonstationarity, or non-Gaussianity of the confounder  $U_i$  or noise  $\epsilon_i$ . In these scenarios, the data generating process was modified as follows from the base process as above but are otherwise the same. Individual observations are indexed by  $i = 1, \dots, n$ .

1. Cubed confounder:  $Y_i \sim N(\beta A_i + U_i^3, \sigma_Y^2)$ .
2. Gamma errors in  $\mathbf{Y}$ :  $Y_i = \beta A_i + U_i + \phi_i$ ,  $\phi_i = q[\Phi(\epsilon_i/\sqrt{3})]$ , where  $q$  is the quantile function for the Gamma(1,  $1/\sqrt{3}$ ) distribution and  $\Phi$  is the standard normal CDF, and  $\epsilon_i \sim N(0, \sigma_Y^2)$ .
3. ‘‘East-west’’ heteroskedasticity:  $Y_i = \beta A_i + U_i + S_{1i} \epsilon_i$ , where  $S_{1i}$  is the first coordinate of  $\mathbf{S}_i$  and  $\epsilon_i \sim N(0, \sigma_Y^2)$ .

4. “Middle-out” heteroskedasticity:  $Y_i = \beta A_i + \sqrt{\frac{\omega(S_{1i})}{3}} U_i + \sqrt{1 - \omega(S_{1i})} \epsilon_i$ , where  $\omega(S_{1i}) = \Phi\left(\frac{S_{1i} - 0.5}{0.1}\right)$  and  $\epsilon_i \sim N(0, \sigma_Y^2)$ .

The last three are borrowed from [Huiying Mao and Reich \(2023\)](#). Five further scenarios were considered.

1. Higher variance in **A**: To illustrate the lessened effect of confounding when there is more independent variation in **A**,  $\sigma_A^2 = 1$ .
2. Very rough processes: To illustrate the difficulty of adjusting for confounding when the unobserved spatial process is very rough, both  $\Sigma_A$  and  $\Sigma_U$  were Matérn correlation matrices with smoothness 0.5, equivalent to exponential correlation.
3. Gridded spatial locations: Theory requires random spatial locations, but this is an illustration of how the method might work with (very regular) fixed spatial locations.
4. Deterministic function of space, same for **A** and **U**: In order to avoid potentially over-stating the effectiveness of DSR when the latent functions of space are both generated and estimated using GPs, the data were generated as:  $Y_i = \beta_0 A_i + g_0(\mathbf{s}_i) + \epsilon_{0i}$ , and  $A_i = m_0(\mathbf{s}_i) + \epsilon_{1i}$ , where  $g_0(\mathbf{s}_i) = m_0(\mathbf{s}_i) = \cos(10s_{i1}) \sin(10s_{i2})$ , and as before  $\epsilon_{0i} \stackrel{i.i.d.}{\sim} N(0, 1^2)$  and  $\epsilon_{1i} \stackrel{i.i.d.}{\sim} N(0, 0.1^2)$ .
5. Deterministic function of space, different for **A** and **U**: Similar to the previous scenario, but now  $g_0(\mathbf{s}_i) = m_0(\mathbf{s}_i) + \sin(10s_{i1}) \sin(10s_{i2})$  and  $m_0$  is defined as in the previous scenario.

Four hundred Monte Carlo replications were performed for each main simulation scenario. Confidence intervals for Spatial+ and gSEM were obtained using 100 nonparametric bootstrap replicates. No adjustment was made in the bootstrapping procedure for spatial correlation between observations, or the tendency of GAMs to under-smooth in bootstrap samples described in [Wood \(2017\)](#). gSEM and Spatial+ used 300 spline basis functions. Methods were compared using their bias, standard error, mean squared error (MSE), coverage, and confidence interval length.

### 3.3 Simulation results

Figure 1 displays sampling distributions of  $\hat{\beta} - \beta_0$  for several illustrative scenarios and a subset of methods. Table 1 displays coverage and mean confidence interval length for each scenario and method displayed in Figure 1. DSR

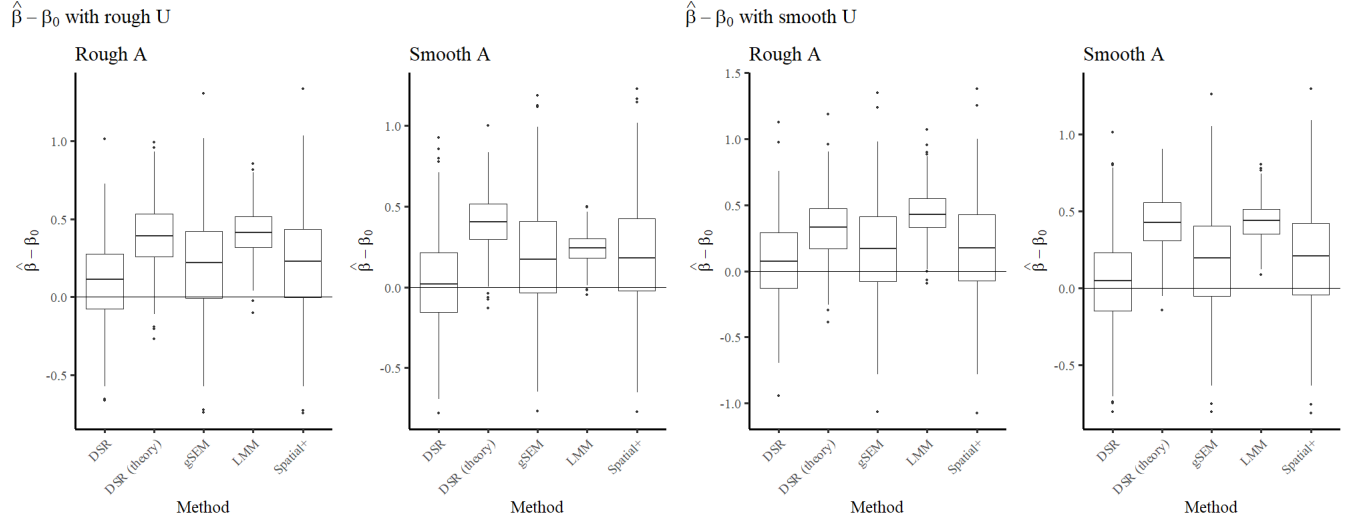


Figure 1: Sampling distribution of  $\hat{\beta} - \beta_0$  from DSR without sample splitting, theoretical DSR, gSEM, LMM, and Spatial+. On the left side, the unobserved confounder  $U$  is smooth, while on the right side it is rough. The smoothness of the treatment variable  $A$  is similarly varied.

is the clear favored method, with lowest bias, and shortest confidence intervals of the methods with at least near-nominal coverage. Theoretical DSR performs fairly poorly in terms of bias, coverage, and confidence interval length. gSEM and Spatial+ are improvements over the linear mixed model, and achieve nominal coverage, but they have higher bias than DSR without sample splitting and have correspondingly wider confidence intervals than DSR. These scenarios were chosen to be particularly challenging cases of spatial confounding, so the linear mixed model performs poorly by all metrics.

$A$	$U$	DSR	Theoretical DSR	gSEM	LMM	Spatial+
Rough	Rough	0.95 (1.14)	0.54 (0.84)	0.95 (1.53)	0.14 (0.51)	0.95 (1.60)
Smooth	Rough	0.96 (1.23)	0.45 (0.78)	0.95 (1.55)	0.24 (0.35)	0.95 (1.62)
Rough	Smooth	0.93 (1.13)	0.66 (0.83)	0.95 (1.53)	0.24 (0.63)	0.95 (1.58)
Smooth	Smooth	0.97 (1.30)	0.42 (0.78)	0.96 (1.55)	0.08 (0.45)	0.96 (1.62)

Table 1: Coverage (mean confidence interval length) of 95% confidence intervals DSR without sample splitting, theoretical DSR, gSEM, LMM, and Spatial+ in illustrative scenarios. Scenarios varied by the smoothness of the treatment variable  $A$  and the unobserved spatial confounder  $U$ .

Full simulation result tables are in the Appendix tables A1-A13. These include the non-Gaussian/non-stationary scenarios, in which DSR continued to perform well. In some scenarios, especially the deterministic scenarios,

using cross-fitting reduced bias and improved coverage of the DSR estimators. DSR implemented with spline regression without cross-fitting outperformed gSEM in many scenarios, indicating that direct estimation of  $g_0(\mathbf{S}_i)$  rather than  $h_0(\mathbf{S}_i)$ , which marginalizes over the distribution of  $A_i$ , improves performance. In the two deterministic scenarios, gSEM is slightly preferred when  $g_0 = m_0$ , but DSR is slightly preferred when  $g_0 \neq m_0$ , perhaps confirming that DSR’s strength is in its estimate of the separate spatial trends. In some scenarios where  $\mathbf{A}$  and  $\mathbf{U}$  were generated using GPs, DSR was able to remove almost all of the confounding bias, but in the deterministic scenarios performance suffered relative to the GP scenarios, although these situations likely correspond to more severe confounding scenarios than the others due to the particular functions chosen, as indicated by the generally higher bias across methods. For example, the LMM had estimated bias of 0.96 and 0.87 in the two deterministic scenarios, about twice the estimated bias in other scenarios.

The confounding scenario in which  $\mathbf{A}$  and  $\mathbf{U}$  were generated according to exponential covariance proved too difficult for any method to perform well and all suffered from substantial bias (Table A10). Among the scenarios in which an adjustment for spatial confounding appeared possible, the ones in which DSR appeared to have a somewhat substantial drawback was when  $\sigma_A^2 = 1$ , in which DSR without sample splitting had coverage of 0.90, as opposed to the nominal 0.95, and had higher bias than gSEM and the shift estimand, although all methods had low bias in this scenario; and the deterministic scenarios, in which DSR with cross-fitting suffered from coverage of about 0.80 in the first deterministic scenario and about 0.90 in the second, with somewhat worse coverage for the estimator without sample-splitting, although bias was competitive with or better than other methods.

## 4 Discussion

Double spatial regression (DSR) is a method to estimate linear regression coefficients using point-referenced data that may be spatially confounded. In simulated confounding scenarios in which the standard spatial regression models suffered from high bias and low coverage, DSR greatly reduced bias, typically achieved nominal or near-nominal coverage, and with the exception of under-coverage in some scenarios and inability of any method to perform well in scenarios with very rough spatial confounders, outperformed other competing methods in many scenarios. We derived explicit regularity conditions that govern asymptotic performance of a slightly different DSR estimator. These regularity conditions are fairly unrestrictive but this “theoretical DSR” estimator performed poorly in simulations with finite samples. DSR also allows closed-form variance estimation, which many competing

methods have lacked. Cross-fitting appeared important to bias and coverage particularly in confounding scenarios that appeared most difficult, such as the scenarios with deterministic functions of space, which tended to increase bias across methods due to the particular functions chosen.

We linked the problem of spatial confounding to existing results in the semiparametric regression literature, which has provided insight into why gSEM is able to reduce bias compared to the naive spatial linear mixed model, and provided Double Machine Learning estimators (which we termed Double Spatial Regression in our narrower application) that outperform others proposed so far. These existing results explain when and why these types of two-stage estimators are able to correct for bias, even when the initial nonparametric regression estimates converge to the true functions slowly. Our results differ from some of those of [Khan and Berrett \(2023\)](#), who found no bias reduction from gSEM compared to the LMM. One possible cause may be the simulation settings used. The exponential covariance used in the simulations of [Khan and Berrett \(2023\)](#) when generating spatially-correlated data results in very rough sample paths, and makes adjusting for resulting confounding bias very difficult. In our simulations using somewhat smoother latent functions of space, both gSEM and DSR improve inference over the LMM, but with exponential covariances, no adjustment performed well (Table A10), and gSEM had worse bias than the LMM, although DSR did not. Simulation results indicate that both use of GP regression using Matèrn covariance, and direct estimation of the function  $g_0$ , as opposed to  $h_0$ , which marginalizes over the distribution of  $A_i$ , reduced DSR's bias compared to gSEM many of our simulated scenarios.

Our method is similar in some ways to that studied in [Gilbert et al. \(2021\)](#), which used a double machine learning-based estimator to nonparametrically estimate the average effect of a shift in a treatment variable under spatial confounding, using bootstrapping to estimate variance. This estimator was naturally well-suited to estimating the average treatment effect when treatment effects were heterogeneous. In many practical situations there are multiple treatment variables, and it is reasonable to assume a linear and additive association between treatment(s) and response. In this situation, DSR is able to estimate multiple linear regression coefficients jointly, with their covariance matrix in closed-form, and with somewhat less variance and MSE than a strictly nonparametric estimate as in [Gilbert et al. \(2021\)](#) (Table A9). The shift estimand exhibited lower bias than DSR in this scenario, but DSR and most methods exhibited low bias in this case. [Gilbert et al. \(2021\)](#) assumed increasing-domain asymptotics, while we assumed a fixed spatial domain.

[Gilbert et al. \(2021\)](#) also suggested using spatially-independent sample splits for cross-fitting, under an assump-

tion of local spatial covariance. With this type of sample splitting, the conditional mean or density functions of the response and treatment variables, conditional on spatial location, are estimated using points in one subset of the spatial domain, and those functions' realized values estimated on a different subset of the spatial domain such that the points in the prediction set are spatially independent from the points in the training set. It is not clear that these estimates can converge to their true values when the training and prediction sets are spatially independent, since the goal is to learn functions of space; deriving conditions on the covariance functions generating the spatially-dependent data that are sufficient to achieve root- $n$  asymptotic normality and consistency when using spatially-independent splits could verify when this strategy can be used.

Further research could analyze convergence rates of functions estimated with Gaussian processes, when hyperparameters are selected using maximum likelihood or REML rather than training-validation splits; the only work we are aware of doing this, although with noiseless observations, is [Karvonen et al. \(2020\)](#). This would help yield more explicit regularity conditions for the main DSR estimator we proposed (although we also proposed using the Vecchia approximation to the full likelihood). DSR could also be extended to use estimating equations of the type proposed by [Robins et al. \(2017\)](#), which require even less regularity of the latent functions. Approaches to areal data should also be investigated. Finally, extensions to other types of semiparametric models, including weighted and nonlinear regression, are discussed in [Robinson \(1988\)](#), [Andrews \(1994\)](#), and [Chernozhukov et al. \(2018\)](#).

## 5 Acknowledgements

Nate Wiecha is supported by the GenX Exposure study, on United States Environmental Protection Agency Superfund grant number P42 ES031009. This work was supported by National Institutes of Health grant R01ES031651-03.

## References

- Andrews, D. W. K. (1994) Asymptotics for semiparametric econometric models via stochastic equicontinuity. *Econometrica*, **62**, 43–72. URL <http://www.jstor.org/stable/2951475>.
- Belloni, A., Chernozhukov, V., Fernández-Val, I. and Hansen, C. (2017) Program evaluation and causal inference with high-dimensional data. *Econometrica*, **85**, 233–298. URL <http://www.jstor.org/stable/44155422>.

- Chernozhukov, V., Chetverikov, D., Demirer, M., Duflo, E., Hansen, C., Newey, W. and Robins, J. (2018) Double/debiased machine learning for treatment and structural parameters. *The Econometrics Journal*, **21**, C1–C68. URL <https://doi.org/10.1111/ectj.12097>.
- Chipman, H. A., George, E. I. and McCulloch, R. E. (2010) BART: Bayesian additive regression trees. *The Annals of Applied Statistics*, **4**, 266 – 298. URL <https://doi.org/10.1214/09-AOAS285>.
- Clayton, D. G., Bernardinelli, L. and Montomoli, C. (1993) Spatial Correlation in Ecological Analysis. *International Journal of Epidemiology*, **22**, 1193–1202. URL <https://doi.org/10.1093/ije/22.6.1193>.
- Cressie, N. A. (1993) *Statistics for Spatial Data*. Wiley, 2 edn.
- Dorie, V. (2024) *dbarts: Discrete Bayesian Additive Regression Trees Sampler*. URL <https://CRAN.R-project.org/package=dbarts>. R package version 0.9-26.
- Dupont, E., Marques, I. and Kneib, T. (2023) Demystifying spatial confounding. *arXiv preprint arXiv:2309.16861*. URL <https://arxiv.org/abs/2309.16861>.
- Dupont, E., Wood, S. N. and Augustin, N. H. (2022) Spatial+: A novel approach to spatial confounding. *Biometrics*, **78**, 1279–1290. URL <https://onlinelibrary.wiley.com/doi/abs/10.1111/biom.13656>.
- Eberts, M. and Steinwart, I. (2013) Optimal regression rates for SVMs using Gaussian kernels. *Electronic Journal of Statistics*, **7**, 1 – 42. URL <https://doi.org/10.1214/12-EJS760>.
- Fuhr, J., Berens, P. and Papies, D. (2024) Estimating causal effects with double machine learning—a method evaluation. *arXiv preprint arXiv:2403.14385*. URL <https://arxiv.org/abs/2403.14385>.
- Gilbert, B., Datta, A., Casey, J. A. and Ogburn, E. L. (2021) A causal inference framework for spatial confounding. *arXiv preprint arXiv:2112.14946*. URL <https://arxiv.org/abs/2112.14946>.
- Gilbert, B., Ogburn, E. L. and Datta, A. (2023) Consistency of common spatial estimators under spatial confounding. *arXiv preprint arXiv:2308.12181*. URL <https://arxiv.org/abs/2308.12181>.
- Guan, Y., Page, G. L., Reich, B. J., Ventrucci, M. and Yang, S. (2022) Spectral adjustment for spatial confounding. *Biometrika*, **110**, 699–719. URL <https://doi.org/10.1093/biomet/asac069>.
- Guinness, J. (2018) Permutation and grouping methods for sharpening gaussian process approximations. *Technometrics*, **60**, 415–429. URL <https://doi.org/10.1080/00401706.2018.1437476>. PMID: 31447491.
- Hodges, J. S. and Reich, B. J. (2010) Adding spatially-correlated errors can mess up the fixed effect you love. *The American Statistician*, **64**, 325–334. URL <https://doi.org/10.1198/tast.2010.10052>.
- Huiying Mao, R. M. and Reich, B. J. (2023) Valid model-free spatial prediction. *Journal of the American Statistical Association*, **0**, 1–11. URL <https://doi.org/10.1080/01621459.2022.2147531>.
- Kanagawa, M., Hennig, P., Sejdinovic, D. and Sriperumbudur, B. K. (2018) Gaussian processes and kernel methods: A review on connections and equivalences. *arXiv preprint arXiv:1807.02582*. URL <https://arxiv.org/abs/1807.02582>.

- Karvonen, T., Wynne, G., Tronarp, F., Oates, C. and Särkkä, S. (2020) Maximum likelihood estimation and uncertainty quantification for gaussian process approximation of deterministic functions. *SIAM/ASA Journal on Uncertainty Quantification*, **8**, 926–958. URL <https://doi.org/10.1137/20M1315968>.
- Khan, K. and Berrett, C. (2023) Re-thinking spatial confounding in spatial linear mixed models. *arXiv preprint arXiv:2301.05743*. URL <https://arxiv.org/abs/2301.05743>.
- Marques, I., Kneib, T. and Klein, N. (2022) Mitigating spatial confounding by explicitly correlating gaussian random fields. *Environmetrics*, **33**, e2727. URL <https://onlinelibrary.wiley.com/doi/abs/10.1002/env.2727>.
- Paciorek, C. J. (2010) The importance of scale for spatial-confounding bias and precision of spatial regression estimators. *Statistical Science*, **25**, 107–125. URL <http://www.jstor.org/stable/41059000>.
- R Core Team (2023) *R: A Language and Environment for Statistical Computing*. R Foundation for Statistical Computing, Vienna, Austria. URL <https://www.R-project.org/>.
- Rasmussen, C. E. and Williams, C. K. I. (2005) *Gaussian Processes for Machine Learning*. The MIT Press. URL <https://doi.org/10.7551/mitpress/3206.001.0001>.
- Reich, B. J., Hodges, J. S. and Zadnik, V. (2006) Effects of residual smoothing on the posterior of the fixed effects in disease-mapping models. *Biometrics*, **62**, 1197–1206. URL <http://www.jstor.org/stable/4124542>.
- Ribeiro Jr, P. J., Diggle, P., Christensen, O., Schlather, M., Bivand, R. and Ripley, B. (2023) *geoR: Analysis of Geostatistical Data*. URL <https://CRAN.R-project.org/package=geoR>. R package version 1.9-3.
- Rice, J. (1986) Convergence rates for partially splined models. *Statistics & Probability Letters*, **4**, 203–208. URL <https://www.sciencedirect.com/science/article/pii/0167715286900672>.
- Robins, J. M., Li, L., Mukherjee, R., Tchetgen, E. T. and van der Vaart, A. (2017) Minimax estimation of a functional on a structured high-dimensional model. *The Annals of Statistics*, **45**, 1951–1987. URL <http://www.jstor.org/stable/26362891>.
- Robinson, P. M. (1988) Root-n-consistent semiparametric regression. *Econometrica*, **56**, 931–954. URL <http://www.jstor.org/stable/1912705>.
- Schlather, M., Malinowski, A., Menck, P. J., Oesting, M. and Storkorb, K. (2015) Analysis, simulation and prediction of multivariate random fields with package randomfields. *Journal of Statistical Software*, **63**, 1–25. URL <https://www.jstatsoft.org/index.php/jss/article/view/v063i08>.
- Schnell, P. M. and Papadogeorgou, G. (2020) Mitigating unobserved spatial confounding when estimating the effect of supermarket access on cardiovascular disease deaths. *The Annals of Applied Statistics*, **14**, 2069 – 2095. URL <https://doi.org/10.1214/20-AOAS1377>.
- Stein, M. (1999) *Interpolation of Spatial Data: Some Theory for Kriging*. Springer Series in Statistics. Springer New York. URL [https://books.google.com/books?id=5n\\_XuL2Wx1EC](https://books.google.com/books?id=5n_XuL2Wx1EC).
- Thaden, H. and Kneib, T. (2018) Structural equation models for dealing with spatial confounding. *The American Statistician*, **72**, 239–252. URL <https://doi.org/10.1080/00031305.2017.1305290>.

Vecchia, A. V. (1988) Estimation and model identification for continuous spatial processes. *Journal of the Royal Statistical Society. Series B (Methodological)*, **50**, 297–312. URL <http://www.jstor.org/stable/2345768>.

Wood, S. N. (2011) Fast stable restricted maximum likelihood and marginal likelihood estimation of semiparametric generalized linear models. *Journal of the Royal Statistical Society: Series B (Statistical Methodology)*, **73**, 3–36. URL <https://rss.onlinelibrary.wiley.com/doi/abs/10.1111/j.1467-9868.2010.00749.x>.

— (2017) *Generalized additive models: an introduction with R, Second Edition*. CRC press.

## 6 Appendix A: Full simulation results

In the following tables, the following methods were compared:

- OLS: ordinary least squares regression.
- LMM: Spatial linear mixed model, estimated using  $G_p G_p$  (Guinness, 2018).
- Spline (GCV): spline model estimated using `mgcv` (Wood, 2011), with smoothing parameter selected by generalized cross-validation, to minimize out-of-sample prediction error.
- Spline (REML): spline model estimated using `mgcv`, smoothing parameter selected by restricted maximum likelihood (REML); Wood (2017) states that this might reduce bias when the parametric component is collinear with smooth term.
- Spatial+: the method of Dupont et al. (2022).
- gSEM: the point-referenced version of Thaden and Kneib (2018), described in Algorithm 1.
- Shift (BART): the shift estimand implemented in Gilbert et al. (2021), using Bayesian Additive Regression Trees (Chipman et al., 2010), or BART, to obtain the preliminary nonparametric estimates. BART estimates were obtained from the R package `dbarts` Dorie (2024). Results only presented in Table A9 due to inability to obtain estimates in other scenarios. Variance estimates not obtained due to relatively high expense of bootstrapping.
- DSR (theory): the alternative/theoretical DSR estimator described in Algorithm 4.
- DSR (theory, no crossfit): the alternative DSR estimator described in Algorithm 4 but without crossfitting.
- DSR: The DSR estimator with crossfitting described in Algorithm 2.
- DSR: (no crossfit): the DSR estimator without crossfitting described in Algorithm 3.
- DSR (spline, no crossfit): the DSR estimator without crossfitting described in Algorithm 3 but with splines used instead of GP regression.

- DSR (theory, spline, no crossfit): the alternative DSR estimator described in Algorithm 4 but without crossfitting, and with splines used instead of GP regression. This is equivalent to the implementation of gSEM used, except that it has a closed-form variance estimate.

The following metrics were used to compare the methods:

- Bias: average difference between estimates and  $\beta_0$  over the Monte Carlo iterations. In all simulations  $\beta_0 = 0.5$ .
- Rel. Bias: relative bias, equal to bias divided by  $\beta_0$ .
- Monte Carlo SE: standard error of bias estimates over the Monte Carlo iterations.
- MSE: mean squared error of estimates over the Monte Carlo iterations.
- 95% CI Length: length of 95% confidence interval.
- 95% CI CVG: coverage, i.e. proportion of Monte Carlo iterations in which the 95% confidence interval included  $\beta_0$ .
- Power: Proportion of Monte Carlo iterations in which the 95% confidence interval did not include 0.

	Bias	Rel. Bias	Monte Carlo SE	MSE	95% CI Length	95% CI CVG	Power
OLS	0.509	1.018	0.016	0.355	0.197	0.068	0.995
LMM	0.417	0.833	0.007	0.194	0.506	0.138	1.000
Spline (GCV)	0.403	0.807	0.007	0.184	0.544	0.205	1.000
Spline (REML)	0.408	0.817	0.007	0.188	0.534	0.180	1.000
Spatial+	0.218	0.437	0.016	0.153	1.604	0.953	0.388
gSEM	0.212	0.424	0.016	0.148	1.534	0.953	0.442
DSR (theory)	0.398	0.795	0.010	0.199	0.838	0.542	0.990
DSR (theory, no crossfit)	0.394	0.788	0.011	0.208	0.923	0.630	0.970
DSR	<b>0.098</b>	0.197	0.013	0.081	1.147	0.948	0.562
DSR (no crossfit)	0.101	0.202	0.013	0.081	1.136	0.945	0.573
DSR (spline, no crossfit)	0.122	0.243	0.013	<b>0.079</b>	1.053	0.940	0.650
DSR (theory, spline, no crossfit)	0.212	0.424	0.016	0.148	1.310	0.912	0.578

Table A1: Simulation results for rough **U** and rough **A**.

	Bias	Rel. Bias	Monte Carlo SE	MSE	95% CI Length	95% CI CVG	Power
OLS	0.359	0.719	0.010	0.169	0.165	0.068	1.000
LMM	0.238	0.476	0.004	0.065	0.348	0.240	1.000
Spline (GCV)	0.225	0.449	0.004	0.058	0.348	0.280	1.000
Spline (REML)	0.226	0.451	0.004	0.059	0.337	0.275	1.000
Spatial+	0.202	0.404	0.017	0.155	1.618	0.948	0.348
gSEM	0.189	0.378	0.017	0.146	1.550	0.945	0.385
DSR (theory)	0.403	0.807	0.009	0.192	0.778	0.452	0.998
DSR (theory, no crossfit)	0.392	0.785	0.012	0.207	0.883	0.595	0.988
DSR	<b>0.027</b>	0.053	0.015	0.093	1.290	0.965	0.378
DSR (no crossfit)	0.033	0.067	0.015	0.086	1.234	0.960	0.410
DSR (spline, no crossfit)	0.093	0.187	0.010	<b>0.052</b>	0.826	0.917	0.800
DSR (theory, spline, no crossfit)	0.189	0.378	0.017	0.146	1.327	0.907	0.522

Table A2: Simulation results for rough **U** and smooth **A**.

	Bias	Rel. Bias	Monte Carlo SE	MSE	95% CI Length	95% CI CVG	Power
OLS	0.511	1.022	0.014	0.341	0.214	0.043	0.995
LMM	0.439	0.879	0.009	0.224	0.635	0.235	1.000
Spline (GCV)	0.463	0.925	0.010	0.255	0.700	0.280	0.998
Spline (REML)	0.458	0.915	0.010	0.250	0.709	0.300	0.998
Spatial+	0.182	0.364	0.018	0.169	1.580	0.953	0.390
gSEM	0.173	0.346	0.018	0.163	1.529	0.953	0.392
DSR (theory)	0.321	0.642	0.011	0.150	0.833	0.655	0.965
DSR (theory, no crossfit)	0.305	0.610	0.012	0.151	0.903	0.718	0.940
DSR	<b>0.082</b>	0.163	0.015	0.100	1.140	0.930	0.537
DSR (no crossfit)	0.086	0.171	0.015	<b>0.100</b>	1.130	0.930	0.532
DSR (spline, no crossfit)	0.120	0.239	0.015	0.100	1.043	0.877	0.632
DSR (theory, spline, no crossfit)	0.173	0.346	0.018	0.163	1.282	0.877	0.537

Table A3: Simulation results for smooth **U** and rough **A**.

	Bias	Rel. Bias	Monte Carlo SE	MSE	95% CI Length	95% CI CVG	Power
OLS	0.485	0.971	0.010	0.277	0.170	0.028	1.000
LMM	0.426	0.851	0.006	0.197	0.453	0.078	1.000
Spline (GCV)	0.422	0.844	0.007	0.195	0.464	0.100	1.000
Spline (REML)	0.421	0.843	0.007	0.194	0.472	0.105	1.000
Spatial+	0.198	0.397	0.018	0.164	1.622	0.958	0.368
gSEM	0.183	0.365	0.017	0.153	1.549	0.960	0.420
DSR (theory)	0.421	0.841	0.009	0.210	0.783	0.420	0.995
DSR (theory, no crossfit)	0.387	0.774	0.011	0.195	0.879	0.562	0.983
DSR	<b>0.013</b>	0.027	0.016	0.101	1.372	0.973	0.358
DSR (no crossfit)	0.033	0.066	0.015	0.095	1.301	0.965	0.405
DSR (spline, no crossfit)	0.170	0.340	0.011	<b>0.080</b>	0.835	0.855	0.855
DSR (theory, spline, no crossfit)	0.183	0.365	0.017	0.153	1.318	0.915	0.537

Table A4: Simulation results for smooth U and smooth A.

	Bias	Rel. Bias	Monte Carlo SE	MSE	95% CI Length	95% CI CVG	Power
OLS	0.163	0.327	0.004	0.035	0.106	0.090	1.000
LMM	0.149	0.299	0.004	0.027	0.233	0.348	1.000
Spline (GCV)	0.147	0.293	0.004	0.027	0.264	0.412	1.000
Spline (REML)	0.148	0.296	0.004	0.028	0.249	0.372	1.000
Spatial+	0.140	0.281	0.013	0.085	1.138	0.943	0.605
gSEM	0.127	0.254	0.012	0.078	1.082	0.943	0.625
DSR (theory)	0.222	0.444	0.007	0.067	0.546	0.630	1.000
DSR (theory, no crossfit)	0.209	0.419	0.008	0.070	0.618	0.740	0.993
DSR	-0.005	-0.009	0.011	0.051	0.892	0.958	0.595
DSR (no crossfit)	<b>0.003</b>	0.005	0.011	0.047	0.849	0.950	0.627
DSR (spline, no crossfit)	0.048	0.096	0.008	<b>0.027</b>	0.582	0.932	0.935
DSR (theory, spline, no crossfit)	0.127	0.254	0.012	0.078	0.931	0.912	0.750

Table A5: Simulation results for middle-out heteroskedastic errors.

	Bias	Rel. Bias	Monte Carlo SE	MSE	95% CI Length	95% CI CVG	Power
OLS	1.503	3.005	0.049	3.205	0.428	0.020	0.993
LMM	0.486	0.973	0.013	0.307	1.044	0.535	0.943
Spline (GCV)	0.453	0.906	0.016	0.309	1.149	0.625	0.882
Spline (REML)	0.509	1.017	0.016	0.358	1.119	0.535	0.932
Spatial+	0.120	0.239	0.016	0.122	1.651	0.983	0.270
gSEM	0.082	0.164	0.015	0.102	1.553	0.988	0.270
DSR (theory)	0.971	1.942	0.026	1.219	1.171	0.168	0.993
DSR (theory, no crossfit)	0.777	1.553	0.022	0.799	1.165	0.300	0.980
DSR	<b>0.079</b>	0.158	0.015	<b>0.097</b>	1.270	0.935	0.450
DSR (no crossfit)	0.098	0.196	0.015	0.097	1.207	0.938	0.520
DSR (spline, no crossfit)	0.279	0.558	0.014	0.158	0.801	0.640	0.897
DSR (theory, spline, no crossfit)	0.082	0.164	0.015	0.102	1.254	0.943	0.465

Table A6: Simulation results for cubed confounder.

	Bias	Rel. Bias	Monte Carlo SE	MSE	95% CI Length	95% CI CVG	Power
OLS	0.403	0.807	0.010	0.201	0.166	0.045	1.000
LMM	0.366	0.732	0.007	0.151	0.423	0.122	1.000
Spline (GCV)	0.361	0.722	0.007	0.149	0.453	0.162	1.000
Spline (REML)	0.363	0.725	0.007	0.150	0.447	0.155	1.000
Spatial+	0.183	0.367	0.018	0.166	1.601	0.963	0.400
gSEM	0.168	0.337	0.018	0.155	1.537	0.955	0.402
DSR (theory)	0.393	0.786	0.009	0.188	0.784	0.480	0.998
DSR (theory, no crossfit)	0.364	0.729	0.011	0.181	0.882	0.640	0.973
DSR	<b>0.010</b>	0.021	0.016	0.106	1.339	0.980	0.390
DSR (no crossfit)	0.024	0.048	0.016	0.100	1.275	0.970	0.428
DSR (spline, no crossfit)	0.140	0.279	0.012	<b>0.073</b>	0.831	0.860	0.807
DSR (theory, spline, no crossfit)	0.168	0.337	0.018	0.155	1.316	0.912	0.525

Table A7: Simulation results for gamma-distributed errors.

	Bias	Rel. Bias	Monte Carlo SE	MSE	95% CI Length	95% CI CVG	Power
OLS	0.234	0.467	0.006	0.069	0.150	0.075	1.000
LMM	0.216	0.432	0.005	0.055	0.331	0.292	1.000
Spline (GCV)	0.215	0.430	0.005	0.056	0.365	0.372	1.000
Spline (REML)	0.217	0.434	0.005	0.057	0.347	0.355	1.000
Spatial+	0.172	0.344	0.018	0.162	1.613	0.955	0.352
gSEM	0.160	0.321	0.018	0.153	1.532	0.948	0.392
DSR (theory)	0.339	0.677	0.009	0.148	0.776	0.613	0.993
DSR (theory, no crossfit)	0.331	0.662	0.012	0.165	0.879	0.677	0.958
DSR	-0.008	-0.015	0.016	0.105	1.294	0.968	0.338
DSR (no crossfit)	<b>0.002</b>	0.005	0.016	0.098	1.229	0.960	0.398
DSR (spline, no crossfit)	0.074	0.147	0.011	<b>0.055</b>	0.826	0.930	0.762
DSR (theory, spline, no crossfit)	0.160	0.321	0.018	0.153	1.322	0.907	0.485

Table A8: Simulation results for east-west heteroskedastic errors.

	Bias	Rel. Bias	Monte Carlo SE	MSE	95% CI Length	95% CI CVG	Power
OLS	0.234	0.467	0.005	0.065	0.120	0.043	1
LMM	0.026	0.051	0.002	0.002	0.124	0.865	1
Spline (GCV)	0.027	0.053	0.002	0.002	0.124	0.858	1
Spline (REML)	0.025	0.049	0.002	0.002	0.124	0.863	1
Spatial+	0.020	0.041	0.002	0.002	0.161	0.965	1
gSEM	0.003	0.005	0.002	0.001	0.163	0.975	1
Shift (BART)	<b>-0.002</b>	-0.004	0.002	0.002	-	-	-
DSR (theory)	0.011	0.023	0.002	0.001	0.124	0.927	1
DSR (theory, no crossfit)	0.007	0.015	0.002	0.001	0.123	0.940	1
DSR	0.009	0.017	0.002	0.001	0.115	0.915	1
DSR (no crossfit)	0.010	0.020	0.002	0.001	0.115	0.900	1
DSR (spline, no crossfit)	0.009	0.017	0.002	0.001	0.115	0.912	1
DSR (theory, spline, no crossfit)	0.003	0.005	0.002	<b>0.001</b>	0.123	0.943	1

Table A9: Simulation results for  $\sigma_A^2 = 1$ . Note the shift estimand considered in [Gilbert et al. \(2021\)](#) is included, without variance estimates.

	Bias	Rel. Bias	Monte Carlo SE	MSE	95% CI Length	95% CI CVG	Power
OLS	0.500	1.000	0.009	0.279	0.174	0.007	1
LMM	0.474	0.948	0.003	0.229	0.273	0.000	1
Spline (GCV)	0.473	0.946	0.004	0.228	0.283	0.000	1
Spline (REML)	0.475	0.950	0.004	0.231	0.268	0.000	1
Spatial+	0.600	1.200	0.006	0.376	0.610	0.005	1
gSEM	0.581	1.162	0.006	0.353	0.603	0.007	1
DSR (theory)	0.487	0.974	0.004	0.244	0.326	0.000	1
DSR (theory, no crossfit)	0.543	1.086	0.007	0.312	0.358	0.000	1
DSR	<b>0.440</b>	0.880	0.005	<b>0.205</b>	0.373	0.018	1
DSR (no crossfit)	0.441	0.881	0.005	0.205	0.374	0.015	1
DSR (spline, no crossfit)	0.451	0.903	0.005	0.214	0.380	0.000	1
DSR (theory, spline, no crossfit)	0.581	1.162	0.006	0.353	0.460	0.000	1

Table A10: Simulation results for very rough, exponential spatial processes generating  $\mathbf{U}$  and  $\mathbf{A}$ .

	Bias	Rel. Bias	Monte Carlo SE	MSE	95% CI Length	95% CI CVG	Power
OLS	0.474	0.948	0.010	0.263	0.172	0.025	1.000
LMM	0.422	0.843	0.007	0.196	0.447	0.080	1.000
Spline (GCV)	0.419	0.837	0.007	0.196	0.456	0.100	1.000
Spline (REML)	0.417	0.834	0.007	0.195	0.463	0.090	1.000
Spatial+	0.185	0.371	0.018	0.166	1.585	0.945	0.380
gSEM	0.170	0.339	0.018	0.154	1.521	0.953	0.385
DSR (theory)	0.429	0.857	0.009	0.218	0.766	0.378	0.993
DSR (theory, no crossfit)	0.385	0.771	0.011	0.195	0.863	0.588	0.978
DSR	-0.003	-0.006	0.017	0.114	1.390	0.953	0.345
DSR (no crossfit)	<b>-0.003</b>	-0.005	0.017	0.114	1.391	0.953	0.340
DSR (spline, no crossfit)	0.164	0.328	0.011	<b>0.080</b>	0.814	0.825	0.848
DSR (theory, spline, no crossfit)	0.170	0.339	0.018	0.154	1.296	0.905	0.498

Table A11: Simulation results for spatial locations located on a regular grid.

	Bias	Relative Bias	Monte Carlo SE	MSE	95% CI Length	95% CI Coverage	Power
OLS	0.958	1.915	0.003	0.921	0.245	0.000	1.000
LMM	0.955	1.910	0.003	0.916	0.251	0.000	1.000
Spline (GCV)	0.955	1.910	0.003	0.916	0.251	0.000	1.000
Spline (REML)	0.957	1.914	0.003	0.920	0.247	0.000	1.000
Spatial+	0.216	0.432	0.017	0.168	1.600	0.960	0.412
gSEM	<b>0.197</b>	0.395	0.017	0.154	1.515	0.958	0.430
DSR (theory)	0.563	1.126	0.012	0.374	0.997	0.388	0.988
DSR (alt., no crossfit)	0.465	0.930	0.014	0.298	1.086	0.615	0.930
DSR	0.218	0.437	0.016	<b>0.146</b>	1.084	0.833	0.647
DSR (no crossfit)	0.310	0.620	0.014	0.180	0.944	0.715	0.823
DSR (spline)	0.363	0.726	0.011	0.176	0.873	0.618	0.975
DSR (alt., spline)	0.197	0.395	0.017	0.154	1.303	0.900	0.547

Table A12: Simulation results for deterministic latent functions of space  $g_0$  and  $m_0$  such that  $g_0 = m_0$ .

	Bias	Relative Bias	Monte Carlo SE	MSE	95% CI Length	95% CI Coverage	Power
OLS	0.986	1.971	0.003	0.975	0.271	0.000	1.000
LMM	0.871	1.741	0.004	0.764	0.511	0.000	1.000
Spline (GCV)	0.837	1.673	0.005	0.709	0.549	0.000	1.000
Spline (REML)	0.845	1.690	0.004	0.722	0.541	0.000	1.000
Spatial+	0.180	0.360	0.018	0.160	1.617	0.953	0.362
gSEM	0.161	0.322	0.017	0.147	1.524	0.950	0.392
DSR (theory)	0.526	1.051	0.012	0.332	1.003	0.470	0.988
DSR (alt., no crossfit)	0.397	0.794	0.014	0.232	1.086	0.688	0.905
DSR	<b>0.154</b>	0.308	0.015	<b>0.108</b>	1.111	0.892	0.595
DSR (no crossfit)	0.232	0.463	0.013	0.123	0.985	0.818	0.805
DSR (spline)	0.323	0.645	0.012	0.159	0.837	0.652	0.963
DSR (alt., spline)	0.161	0.322	0.017	0.147	1.295	0.905	0.498

Table A13: Simulation results for deterministic latent functions of space  $g_0$  and  $m_0$  such that  $g_0 \neq m_0$ .

## 7 Appendix B: Proof of Theorem 1

Theorem 1 follows from Theorem 4.1 from (Chernozhukov et al., 2018), and Theorems 3.3 and 3.6 from (Eberts and Steinwart, 2013). To apply these theorems, this section establishes that assumptions A1-A6 satisfy the necessary assumptions. For the probability distribution  $P$  with density function  $p(w)$ , and for a function  $f$ ,  $\|f\|_{P,q} := \{\int |f(w)|^q p(w) dw\}^{1/q}$ .

Assumption 1 repeats the assumptions required for Theorem 4.1 from (Chernozhukov et al., 2018). Let  $C, c, q > 4$  be positive constants.  $h$  denotes the function  $h(\mathbf{S}_i) = E(Y_i|\mathbf{S}_i)$ . The observations  $\mathbf{W}_i = (Y_i, A_i, \mathbf{S}_i)$  are assumed

to be i.i.d. from a probability distribution  $P$ .

**Assumption 1** (Regularity conditions for DML partially linear model). *Let  $(\delta_n), (\Delta_n)$  be sequences converging to 0. Assume that:*

- (a) *The data are generated by (1).*
- (b)  $\|Y_i\|_{P,q} + \|A_i\|_{P,q} \leq C$  for all  $i = 1, \dots, n$ .
- (c)  $\|U_i V_i\|_{P,2} \geq c^2$  and  $E_P[V_i^2] \geq c$  for all  $i = 1, \dots, n$ .
- (d)  $\|E_P[U_i^2 | \mathbf{S}_i]\|_{P,\infty} \leq C$  for all  $i = 1, \dots, n$ .
- (e) *Given a random subset  $I$  of  $[n]$  of size  $n/K$ , the nuisance parameter estimator  $\hat{\eta} = \hat{\eta}((\mathbf{W}_i)_{i \in I^c})$  obeys the following conditions for all  $n/K \geq 1$ : with  $P$ -probability no less than  $1 - \Delta_n$ ,*

$$\|\hat{\eta}_0 - \eta_0\|_{P,q} \leq C, \|\hat{\eta}_0 - \eta_0\|_{P,2} \leq \delta_n$$

$$\text{and } \|\hat{m} - m\|_{P,2} \times \left( \|\hat{m} - m\|_{P,2} + \|\hat{h}_0 - h\|_{P,2} \right) \leq \delta_n n^{-1/2}.$$

The following lemma is Theorem 4.1 from (Chernozhukov et al., 2018) restated with DSR estimation substituted for DML estimation. Its conclusion is identical to Theorem 1, but has different assumptions. Theorem 1 is proved by verifying that Assumptions A1-A6 together with estimation by Algorithm 4 satisfy the conditions of Assumption 1 required for Lemma 1.

**Lemma 1** (DSR Inference on Regression Coefficients in the Partially Linear Regression Model). *Suppose Assumption 1 holds. Then the DSR estimator  $\hat{\beta}_0$  and the variance estimator  $\widehat{Var}(\hat{\beta}_0)$  obtained by Algorithm 4 obey  $\widehat{Var}(\hat{\beta}_0)^{-1/2}(\hat{\beta}_0 - \beta_0) \xrightarrow{D} N(0, 1)$ .*

Lemma 2 follows directly from Theorem 3.3 from (Eberts and Steinwart, 2013), using  $\rho = \ln(n)$ . Note that the estimated function from the least-squares SVM with Gaussian kernel and least-squares loss analyzed in (Eberts and Steinwart, 2013) is identical to the posterior mean of a Gaussian process with Gaussian kernel; see e.g. (Kanagawa et al., 2018).

**Lemma 2** (Convergence rate for bounded regression using GP posterior mean). *Let  $\hat{f}$  be an estimate of  $f(S) = E(Y|S)$  obtained by a Gaussian process posterior mean, with Gaussian kernel, using parameters  $\gamma_n, \lambda_n$  selected by the training-validation scheme in (Eberts and Steinwart, 2013) using grids as specified in Algorithm 4. Let  $P_S$  be the marginal distribution of  $S$  over  $\mathbb{R}^d$  with support in the  $\|\cdot\|_2$ -unit ball. Let the density of  $P_S$  be  $p_S \in L_q(\mathbb{R}^d)$  for some  $q \geq 1$ , and let  $f \in L_2(\mathbb{R}^d) \cap L_\infty(\mathbb{R}^d)$  and  $f \in B_{2s,\infty}^\alpha$  for  $\alpha \geq 1$  and  $s \geq 1$  such that  $\frac{1}{q} + \frac{1}{s} = 1$ . Let  $Y \in [-M, M]$ ,  $M > 0$  and let  $\hat{f}$  be clipped at  $-M, M$ .*

*Then with probability no less than  $1 - \frac{1}{n}$ ,  $\|\hat{f} - f\|_{P,2} \leq Cn^{-\frac{\alpha}{2\alpha+d} + \xi}$ , for all  $\xi > 0$  and some  $C > 0$ .*

Lemma 3 follows directly from Theorem 3.6 from (Eberts and Steinwart, 2013), using  $\hat{\rho} = \ln(n)$  and  $\bar{\rho} = \ln(n)$  and clipping the absolute value of the fitted function at  $\min\{1, M_n\}$  rather than simply  $M_n$ , which does not change the result since by assumption the true function lies in  $[-1, 1]$ . Note that per the proof of Theorem 3.6, the constant  $C$  in the original statement of Theorem 3.6 does not depend on either  $\hat{\rho}$  or  $\bar{\rho}$  allowing these substitutions.

**Lemma 3** (Convergence rate for regression with normal errors using GP posterior mean). *Let  $\hat{f}$  be an estimate of  $f(S) = E(Y|S)$  obtained by a Gaussian process posterior mean, with Gaussian kernel, using parameters  $\gamma_n, \lambda_n$  selected by the training-validation scheme in (Eberts and Steinwart, 2013) using grids as specified in Algorithm 4. Let  $P_S$  be the marginal distribution of  $S$  over  $\mathbb{R}^d$  with support in the  $\|\cdot\|_2$ -unit ball. Let the density of  $P_S$  be  $p_S \in L_q(\mathbb{R}^d)$  for some  $q \geq 1$ , and let  $f \in L_2(\mathbb{R}^d) \cap L_\infty(\mathbb{R}^d)$  and  $f \in B_{2s,\infty}^\alpha$  for  $\alpha \geq 1$  and  $s \geq 1$  such that  $\frac{1}{q} + \frac{1}{s} = 1$ . Assume further that  $f(S) \in [-1, 1]$ .*

*Let  $Y_i = f(S_i) + \epsilon_i$  where  $\epsilon_i \sim \text{ind. } N(0, \sigma_i^2)$ , and let there exist some constant  $C_0$  such that all  $\sigma_i^2 < C_0$ . Let  $\hat{f}$  be clipped so that  $|\hat{f}| \leq \min\{1, M_n\}$  where  $M_n = 4\sqrt{C_0}\sqrt{\ln(n)}$ .*

*Then with probability no less than  $1 - \frac{2}{n}$ ,  $\|\hat{f} - f\|_{P,2} \leq Cn^{-\frac{\alpha}{2\alpha+2} + \xi}$ , for all  $\xi > 0$  and some  $C > 0$ .*

The proof of Theorem 1 follows directly from assumptions A1-A6 and Facts 1-3.

*Proof of Theorem 1.* In Assumption 1, (a) follows by assumption A1, (b) follows from the assumption of bounded or normal distributions of  $U_i, V_i | \mathbf{S}_i, A_i$ , a bounded spatial domain  $\mathcal{S}$ , and assumption A4, (c) follows from the assumption of non-zero variance of  $U_i, V_i$ , and  $E(U_i^2 V_i^2)$ , and (d) is satisfied by the assumption of bounded variance of the error terms in A2.

To satisfy (e) in Assumption 1, first note that by assumption both  $\eta_0$  and  $\hat{\eta}_0$  are bounded by some interval, satisfying  $\|\eta_0 - \hat{\eta}_0\|_{P,q} < C$  for some  $C > 0$  and  $q > 4$ . Next apply Lemmas 2 and 3 to satisfy the convergence rate

requirements. If  $\alpha_A > \frac{d}{2}$ , then if  $m_0$  is estimated by  $\hat{m}_0$  using a Gaussian process mean with clipping at appropriate bounds as in the previous two facts, then with probability converging to 1,  $\|\hat{m}_0 - m_0\|_{P,2} \leq C_1 n^{-\frac{\alpha_A}{2\alpha_A+d} + \xi} < C_1 n^{-1/4}$  for any  $\xi > 0$  and therefore  $\|\hat{m}_0 - m_0\|_{P,2}^2 < C_1 n^{-1/2}$ . Then  $\|\hat{m}_0 - m_0\|_{P,2} \leq C_1 n^{-\frac{\alpha_A}{2\alpha_A+d} + \xi}$  for all  $\xi > 0$ .

If  $\alpha_Y > \frac{d^2}{4\alpha_A}$ , then with probability converging to 1,  $\|\hat{g}_0 - g_0\|_{P,2} \leq C_0 n^{-\frac{\alpha_Y}{2\alpha_Y+d} + \xi} < C_0 n^{-\frac{d}{2(2\alpha_A+d)}}$  for some  $C_0 > 0$  and all  $\xi > 0$ .

Then,  $\|\hat{g}_0 - g_0\|_{P,2} \times \|\hat{m}_0 - m_0\|_{P,2} < C_0 n^{-\frac{d}{2(2\alpha_A+d)}} \times C_1 n^{-\frac{\alpha_A}{2\alpha_A+d}} < C n^{-\frac{1}{2}}$  with probability converging to 1.

Thus part (e) of Assumption 1 is satisfied.

With parts (a)-(e) of Assumption 1 satisfied, apply Fact 1 to obtain  $\widehat{Var}(\hat{\beta}_0)^{-1/2}(\hat{\beta}_0 - \beta_0) \xrightarrow{D} N(0, 1)$ .  $\square$

This result can be extended to partially linear regression where the number of independent variables is greater than 1.